Spatial variations of biochemical content and stable isotope ratios of size-fractionated plankton in the Mediterranean Sea (MERITE-HIPPOCAMPE campaign)

Javier Angel Tesán-Onrubia, Marc Tedetti, François Carlotti, Melissa Tenaille, Loic Guilloux, Marc Pagano, Benoit Lebreton, Gaël Guillou, Pamela Fierro-González, Catherine Guigue, et al.

Spatial variations of biochemical content and stable isotope ratios of size-fractionated plankton in the Mediterranean Sea (MERITE-HIPPOCAMPE campaign)

Javier Angel Tesán-Onrubia[a*], Marc Tedetti[a], François Carlotti[a], Melissa Tenaille[a], Loïc Guilloux[a], Marc Pagano[a], Benoit Lebreton[b], Gaël Guillou[b], Pamela Fierro-González[a], Catherine Guigue[a], Sandrine Chifflet[a], Théo Garcia[a], Ismail Boudriga[c], Malika Belhassen[c], Amel Bellaaj Zouari[c], Daniela Bănaru[a*]

[a] Aix Marseille Univ., Université de Toulon, CNRS, IRD, MIO UM 110, 13288, Marseille, France

[b] UMR 7266 Littoral Environnement et Sociétés (CNRS - La Rochelle Université), La Rochelle, France

[c] Institut National des Sciences et Technologies de la Mer (INSTM), 28, rue 2 mars 1934, 24 Salammbô 2025, Tunisia

* Correspondence:
Javier Angel Tesán-Onrubia; javier.tesan@mio.osupytheas.fr
Daniela Bănaru; daniela.banaru@mio.osupytheas.fr

Revised version for submission to Marine Pollution Bulletin – Special issue "Plankton and Contaminants in the Mediterranean Sea: Biological pump and interactions from regional to global approaches"

Abstract

Plankton represents the main source of carbon in marine ecosystems and is consequently an important gateway for contaminants into the marine food webs. During the MERITE–HIPPOCAMPE campaign in the Mediterranean Sea (April-May 2019), plankton was sampled from pumping and net tows at 10 stations from the French coast to the Gulf of Gabès (Tunisia) to obtain different size fractions in contrasted regions. This study combines various approaches, including biochemical analyses, analyses of stable isotope ratios ($\delta^{13}C$, $\delta^{15}N$), cytometry analyses and mixing models (MixSiar) on size-fractions of phyto- and zooplankton from 0.7 to > 2000 µm. Pico- and nanoplankton represented a large energetic resource at the base of pelagic food webs. Proteins, lipids, and stable isotope ratios increased with size in zooplankton and were higher than phytoplankton. Stable isotope ratios suggest different sources of carbon and nutrients at the base of the planktonic food webs depending on the coast and the offshore area. In addition, a link between productivity and trophic pathways was shown, with high trophic levels and low zooplankton biomass recorded in the offshore area. The results of our study highlight spatial variations of the trophic structure within the plankton size-fractions and will contribute to assess the role of the plankton as a biological pump of contaminants.

Keywords: Phytoplankton, zooplankton, $\delta^{13}C$, $\delta^{15}N$, plankton trophic structure, contaminants

1. Introduction

Phyto- and zooplankton play a central role in the functioning of marine ecosystems by producing, transforming and transferring the organic matter up to planktivorous species (Bănaru et al., 2019; Chen et al., 2022). Plankton thus represents the main source of carbon fueling the marine food webs (Bănaru et al., 2013; Cresson et al., 2020). Phyto- and zooplankton are composed of a myriad of organisms of great diversity in terms of size, metabolism, physiology, and diet that are governed by different trophic pathways, and complex ecological interactions. As taxonomic composition strongly differs between planktonic size-fractions, a size-based approach has become widely used to study the structure and functioning of the planktonic compartment (Rau et al., 1990; Rolff, 2000; Carlotti et al., 2008; Hunt et al., 2017). In pelagic food webs, body size determines rates of production (Banse and Mosher, 1980), energy requirements (Brown et al., 2004), mortality rates (Hirst and Kiørboe, 2002) and predator-prey interactions (Cohen et al., 1993; Ljungström et al., 2020). The biochemical composition of the different plankton size-fractions provides information on their energetic content, which may influence prey selection (Carlotti et al., 2008, Harmelin-Vivien et al., 2019; Chen et al., 2019, 2021, 2022), while the carbon and nitrogen isotopic ratios ($\delta^{13}C$ and $\delta^{15}N$ values) of the plankton size-fractions provide information on the fluxes of organic matter within the planktonic food webs (Peterson et al., 1985; Cabana and Rasmussen, 1994; Vander Zanden and Rasmussen, 2001).

Besides its central role in the functioning of marine ecosystems, plankton is now recognized as a key gateway of inorganic and organic contaminants into the marine food web (Tao et al., 2018; Chouvelon et al., 2019; Tedetti et al., 2023). Phytoplankton is exposed to contaminants *via* water. Bioconcentration of contaminants in phytoplankton is driven mainly by partition equilibrium processes between the cells and the surrounding water (Frouin et al., 2013). For a given species or cell size of phytoplankton, and a given physico-chemical habitat (temperature, organic carbon content, etc.), the bioconcentration factors of organic contaminants may be directly correlated with their octanol-water partitioning coefficients (log K_{ow}), i.e., their degree of lipophilicity/hydrophobicity (Frouin et al., 2013). Correspondingly, the bioconcentration of a given contaminant has been shown to increase with decreasing size of phytoplankton (Fan and Reinfelder, 2003). Bioaccumulation processes in zooplankton are highly complex due to the entry of contaminants by both the water aqueous phase (bioconcentration) and diet, the trophic interactions and/or transfers between phytoplankton and various zooplankton, and the contaminant removal processes used by these organisms

(Tiano et al., 2014; Alekseenko et al., 2018; Tao et al., 2018). Biomagnification may also occur between the low and high trophic level organisms in the marine food webs (Chouvelon et al., 2019).

Therefore, the uptake, accumulation, and transfer of contaminants within the planktonic food webs may be strongly influenced by its characteristics such as the size-fraction distribution, the biochemical/energetic content (Hennig, 1986; Mason et al., 1995; Wu and Wang, 2011), the trophic interactions and the fluxes of organic matter (Peterson et al., 1985; Cabana and Rasmussen, 1994; Vander Zanden and Rasmussen, 2001). Characterizing the content of phyto-, and zooplankton in terms of size-fraction, biochemical/energetic content and stable isotope ratios ($\delta^{13}C$ and $\delta^{15}N$) may thus provide key information on the structure, functioning, and trophic interactions of this planktonic food webs, but also on the capacity of accumulation and transfer of organic and inorganic contaminants within this planktonic network and potentially their transfer to higher trophic levels.

The Mediterranean Sea has a high diversity of planktonic and exploited resources, and contrasted biogeographical regions impacted by climate change and human activities (Durrieu de Madron et al., 2011; Mayot et al., 2017). As the Mediterranean Sea is mainly oligotrophic, its autotrophic biomass is dominated by small-size pico- and nanophytoplankton groups (Leblanc et al., 2018; Boudriga et al., 2022). These groups play a key role in the biomass and energy transfer to zooplankton (Bănaru et al., 2014; Hunt et al., 2017; Leblanc et al., 2018). However, coastal areas impacted by riverine and urban inputs may locally be more enriched and sometimes can even be characterized by higher phytoplankton biomass dominated by larger cells such as dinobionts and diatoms (Harmelin-Vivien et al., 2008). Champalbert (1996) highlighted spatial differences in the zooplankton diversity and biomass, with a lower diversity and a higher biomass in coastal waters relative to offshore areas. The Mediterranean Sea is also strongly exposed to chemical contamination due to the intensive human activities in the bordering countries, its semi-closed status that limits the dilution of contaminants, and the relatively short ventilation and residence times its waters (Durrieu de Madron et al., 2011; Tedetti et al., 2023).

In this context, the aims of this work, carried out in the frame of the MERITE-HIPPOCAMPE campaign, were: 1) to investigate the structure and functioning (in terms of trophic interactions and organic matter fluxes) of the planktonic food webs of the Mediterranean Sea through the characterization of the biomass, biochemical/energetic content and $\delta^{13}C/\delta^{15}N$ ratios of several size-fractions of phyto- and zooplankton ranging from 0.7 to > 2000 µm, 2) to explore variations in size-spectra and spatial variations of these characteristics

(biochemical/energetic content and $\delta^{13}C/\delta^{15}N$ ratios), and relate these variations to their composition (*via* cytometry and imagery analyses) and also to the specificities of the studied areas, and 3) to discuss the implications of these findings regarding the accumulation and transfer of contaminants in the planktonic food webs.

To our knowledge, this work represents the first study to use a wide variety of approaches, and methodologies, such as biochemical analyses (proteins, carbohydrates, lipids and energy), analyses of isotopic ratios ($\delta^{13}C$, $\delta^{15}N$), cytometry analyses and mixing models (MixSiar) on fine size-fractions of phyto- and zooplankton ranging from 0.7 to > 2000 µm for the purpose of studying plankton food webs. The use of innovative sampling techniques, such as the deployment of *in situ* pumps equipped with a sequential filtration system, or the towing of a MultiNet device in chlorophyll maximum layer (CML), enabled us to obtain large amounts of size fractionated phyto- and zooplankton, material rarely acquired together.

2. Material and methods

2.1. Study area and sampling

The MERITE-HIPPOCAMPE cruise was conducted in the Mediterranean Sea in spring 2019, from April 13 to May 14, onboard the R/V *Antea* (Tedetti and Tronczynski, 2019; Tedetti et al., 2023). Ten stations were sampled from the French coast (La Seyne-sur-Mer, Northwestern Mediterranean) to the Gulf of Gabès in Tunisia (Southeastern Mediterranean) in coastal and offshore locations, including the Gulf of Lion, the Ligurian and Algerian consensus regions, the North Balearic Front and Sicilian Channel areas, and the gulfs of Hammamet and Gabès, which presented different hydrological, biogeochemical and bloom conditions, and different levels of anthropogenic pressures (Fig. 1, Table S1). Phytoplankton and zooplankton were sampled at each station at the CML, during spring bloom (April to May), when maximum primary and secondary production occurs (Liénart et al., 2018; Tedetti et al., 2023).

Suspended particulate matter (SPM) was collected and filtered using McLane Large Volume Water Transfer System Samplers (WTS6-142LV, 4–8 L min^{-1}), hereinafter referred to as McLane *in situ* pumps. One pump was mounted with a regular 142-mm filter-holder holding one 142-mm-diameter filter. This pump was equipped with a ~ 0.7-µm-pore-size pre-combusted pre-weighed GF/F filter (Whatman) and covered with a 60-µm-pore-size homemade sock-type pre-filter so that the filtered particle size-fraction was 0.7–60 µm. A second McLane *in situ* pump was mounted with a mini-Multiple Unit Large Volume *in situ* Filtration System (MULVFS) filter holder composed of baffle tubes on the top followed by

146 successive baffle and filter support plates, for sequential filtration with three different filters
147 (142-mm diameter) (Bishop et al., 2012). The filter series used were one ~ 0.7-µm-pore-size
148 pre-combusted (450 °C, 6 h), pre-weighed GF/F filter, one 2.7-µm-pore-size pre-combusted,
149 pre-weighed GF/D filter (Whatman), and one 20-µm-pore-size pre-cleaned (HCl 0.05% v/v)
150 pre-weighed home-made Nylon filter so that the filtered particle size fractions were 0.7–2.7,
151 2.7–20, and > 20 µm (hereafter labeled 20–60 µm). The pumps were deployed in the CML
152 between 40 and 60 min. The volumes of filtered seawater ranged between 169 and 300 L
153 depending on the stations. After pump deployment, filters were 'dried' by connecting the filter
154 holder to a vacuum pump, stored in pre-combusted (450 °C, 6 h) aluminum sheets, and
155 conserved at –20 °C and then freeze-dried. Then, punches with a known surface area were
156 made into filters to obtain subsamples for the different analyses.
157 Zooplankton was sampled using a Multinet Plankton Sampler (Midi type with 0.25-m^2
158 aperture, Hydro-Bios), referred to hereafter as 'MultiNet', towed horizontally in the CML. The
159 MultiNet position was maintained stable at the defined layer by means of a V-fin deflector
160 and controlled vessel speed (2.5 knots), and real-time control of its position from the onboard
161 desk-unit. The MultiNet was mounted with five individual (exchangeable) 2.5-m-long nylon
162 nets with a mesh size of 60-µm and cod ends of the same mesh size. The MultiNet frame was
163 equipped with various sensors: two Hydro-Bios flowmeters (one at the mouth and the other
164 on the side) to assess the volume of water filtered by the nets, a CTD sensor and a total
165 chlorophyll *a* (TChl*a*) fluorometer. Connected to the onboard desk unit *via* the electro-
166 mechanical cable, these captors inform on *in situ* depth, TChl*a* concentration, filtered volume
167 and flow rate, allowing the operator to decide to open and close the nets. Nets were closed
168 when the flow rate reached a threshold value to limit clogging. Filtered volumes for each net
169 reached up to 185 m^3. Once the five nets were filled, the MultiNet was hauled back on board,
170 and the five cod ends linked by a helicoidal bucket connector were carefully recovered. The
171 fifth net remained open until the end of the operation, filtering the layer between the CML
172 and the surface. The cod ends were rinsed out with local seawater, and their content
173 transferred to pre-cleaned 10-L PFA bottles. The MultiNet was then returned to the water.
174 This operation was repeated several times to get sufficient amounts of plankton for all
175 possible further contaminant content analyses (Tedetti et al., 2023). In the clean onboard
176 container lab, plankton collected in PFA bottles was then size-fractionated through a column
177 of five stainless steel sieves (60, 200, 500, 1000 and 2000 µm mesh-size) by wet-sieving with
178 seawater previously filtered onto GF/F filters and stored in stainless steel jerrycans to obtain
179 the following size-fractions: 60–200, 200–500, 500–1000, 1000–2000 and > 2000 µm.

Samples were stored in pre-combusted (450 °C, 6 h) Pyrex bottles, conserved at –20 °C and freeze-dried. Large fractions (> 2000 µm) were most likely under-sampled compared to smaller fractions. These fractions should be carefully treated because they represent a relatively low – and difficult to estimate – biomass, form colonies, and may actively evade capture by swimming. The detailed methods to determine zooplankton group composition analysis presented in this paper and related to our results are detailed in Fierro-González et al. (2023).

2.2. Analyses

2.2.1. Particulate organic carbon and nitrogen

Samples (i.e., 22-mm diameter filter or 1 mg dry weight DW zooplankton) were leached with 100 µL of sulfuric acid (H_2SO_4 0.5 mol L^{-1}) to remove any inorganic carbon. Samples were then stored in 25 mL Schott® glass bottles for subsequent analyses. Filter blanks were conditioned with 1 mL of ethanol and with 600 mL of 0.2-µm filtered seawater. Determination of particulate organic carbon (POC) and nitrogen (PON) concentrations were carried out simultaneously on the same sample using the persulfate wet-oxidation procedure according to Raimbault et al. (1999).

2.2.2. Suspended particulate matter and plankton dry weight

Suspended particulate matter dry weight (SPM_{DW}) was measured in the 0.7–60 and 20–60-µm filters gravimetrically by weighing the tare, wet and dry filters with a precision balance (d = 0.01 mg). Briefly, we subtracted from the dry filter the tare and the salts associated with the evaporated water, considering a salinity of 38. Tests conducted with filtered seawater evidenced a higher mass after drying than the salt present in water, and most likely related to the highly hygroscopic characteristics of salts. A ratio of 1.2 between the observed mass and the theoretical mass associated with salt was applied to correct the water bonded to salt. When biomasses were low, as for 0.7–2.7 and 2.7–20-µm filters, high uncertainty in weighing increased the margin of error. SPM_{DW} in the 0.7–2.7 and 2.7–20-µm filters were thus estimated by multiplying their relative fraction of POC by the biomass measured gravimetrically in the 0.7–60-µm size-fraction. POC can be employed as a proxy of SPM_{DW}, based on the correlations assessed by Trimble and Baskaran (2005). SPM_{DW} at the CML is mainly composed of POC (around 50%) but also contains biogenic silica, calcium carbonate and lithogenic matter (Bishop et al., 1977; Krasakopoulou and Karageorgis, 2005). On the

basis of these observations, relative POC was used to assess the contribution of the different size-fractions to the total biomass. Plankton dry weight (Plankton $_{DW}$) of size fractions 60–200, 200–500, 500–1000, 1000–2000, and > 2000 µm were determined after drying samples on pre-weighed GF/F filters (60 °C, 24 h) and then re-weighed with a microbalance, taking into consideration the volumes of water filtered by the MultiNet (Fierro-González et al., 2023).

2.2.3. Biochemical and energy content

Biochemical compounds (proteins, carbohydrates, and lipids) were extracted in triplicate from freeze-dried filters and zooplankton samples and expressed in µg mg^{-1} DW. Absorbance of the extracts was then measured at different wavelengths using a spectrophotometer (Shimadzu, UV-1280). Briefly, proteins were extracted using a Folin phenol reagent following the Lowry et al. (1951) method and measured at 700 nm. Carbohydrates were extracted using the phenol-sulfuric acid reaction described in Dubois et al. (1956) and measured at 490 nm. Finally, lipids were extracted with a monophasic methanol-dichloromethane solution (Bligh and Dyer, 1959) and measured at 360 nm. Ashes and residual organic compounds not recovered by these standard biochemical assays (chitin for example) may be estimated by subtracting the weight of the biochemical compounds from the total dry weight, but were not presented in this study. The energy content (E_i) was estimated by summing the three biochemical compounds after converting them into energetic units (21.4 kJ g^{-1} for proteins, 17.2 kJ g^{-1} for carbohydrates and 35.6 kJ g^{-1} for lipids) (Postel et al., 2000). The plankton energy amount (E_T) provided by plankton per cubic meter per station at CML (kJ m^{-3}) was calculated for all the plankton size-fractions by multiplying the SPM_{DW} or the biomass (B_i in mg DW m^{-3}) of each size-fraction at a given station by its energy content (E_i in kJ mg^{-1} DW) and the sum of E_T of all size-fractions represents the plankton total energy amount, E_{TS}: $E_T = B_i \times E_i$.

2.2.4. Stable isotope analyses ($\delta^{13}C$ and $\delta^{15}N$)

The SPM_{DW} collected on filters was scraped off with a scalpel. Zooplankton samples were ground to a fine powder with an agate mortar and pestle. Presence of carbonates on samples can bias the measurement of $\delta^{13}C$ values as they are enriched in ^{13}C compared to organic matter (Pinnegar and Polunin, 1999). Therefore, samples were acidified prior to the measurement of $\delta^{13}C$ values of the particulate organic matter (POM). Samples were acidified using HCl 1% and immediately rinsed with MilliQ-water. Measurements of $\delta^{15}N$ values of the

POM were carried out on raw samples. For zooplankton, approximately 0.5 mg of powder was weighed into a tin cup (8 × 5 mm) using a precision balance (d = 0.01 mg). Carbon and nitrogen stable isotope analyses were performed using a continuous-flow isotope-ratio mass spectrometer (Delta V Plus, Thermo Scientific) with a Conflo IV interface coupled to an elemental analyzer (EA Isolink, Thermo Scientific). Analyses were conducted at the Littoral, Environment and Societies Joint Research Unit stable isotope facility (CNRS - University of La Rochelle, France). The $\delta^{13}C$ and $\delta^{15}N$ values are expressed in δ notation as deviations from standards (Vienna Pee Dee Belemnite for $\delta^{13}C$ and N_2 in air for $\delta^{15}N$), in ‰, according to the formula:

$$\delta X_{sample} = \left[\left(\frac{R_{sample}}{R_{standard}}\right) - 1\right] x\ 1000$$

where X is ^{13}C or ^{15}N, R_{sample} is the isotopic ratio of the sample and $R_{standard}$ is the isotopic ratio of the standard. Calibration was carried out using reference materials (USGS-61, -62, -63 for both carbon and nitrogen). The analytical precision of the measurements was < 0.10‰ for carbon and nitrogen based on analyses of USGS-61 and USGS-63 used as laboratory internal standards.

2.2.5. Cytometry and imagery analyses

For flow cytometry analyses, seawater was sampled with Niskin and Go-Flo bottles at the CML. Seawater was filtered through a silk mesh filter with 100-µm pore size and then immediately fixed with a 2% paraformaldehyde solution. Samples were incubated for 15 min at 4 °C in the dark and then stored in liquid nitrogen onboard and at –80 °C in the laboratory until analysis. The autotrophic pico- and nanoplankton were analyzed using a CyFlow®Space flow cytometer (SysmexPartec) equipped with a blue diode pumped solid-state laser (20 mW; 488 nm) and a red diode laser (25 mW; 638 nm). Seawater samples were thawed in the dark, filtered through a nylon mesh filter with a porosity of 30 µm (CellTrics®, SysmexPartec), and mixed with flow check high-intensity beads of 2-µm diameter (Polysciences, USA). Cells were characterized based on their scatter and fluorescence signals (Khammari et al., 2018) and data were analyzed with the FloMax software (Sysmex Partec), which directly calculates the cell concentration (cells cm^{-3}) of the resolved cell groups. Carbon biomass of each cell group was estimated according to Khammari et al., (2020). The contributions of zooplankton, phytoplankton (microalgae), and detritus components to the total Plankton $_{DW}$ were estimated

using imagery methods (FlowCAM and ZOOSCAN) according to Fierro-González et al. (2023).

2.3. Bayesian mixing model

The contributions of the different size-fractions of phytoplankton (0.7–2.7, 2.7–20 and 20–60 µm) as food resources to zooplankton size-fractions and their confidence intervals were estimated using a Bayesian mixing model using the R package MIXSIAR (Parnell et al., 2013; https://github.com/brianstock/MixSIAR). This modeling approach incorporates variability of potential food source isotopic compositions for consumers and of trophic fractionation factors (TFF) and generates probability distributions of food source contributions. The consumers (i.e., zooplankton) were grouped in the 60–500, 500–2000, and > 2000-µm size-fractions based on statistical differences in their isotopic compositions. Zooplankton size-fractions with similar isotopic compositions were thus considered to consume the same food resources. Contributions were computed using $\delta^{13}C$ and $\delta^{15}N$ values. As there is no well-established set of TFFs for plankton, we computed mixing model estimates using the mean TFF values of 1.70 ± 0.38 ‰ for $\delta^{13}C$ and 2.40 ± 0.26 ‰ for $\delta^{15}N$ (mean ± standard error (SE)), as established by Tiselius and Fransson (2016).

2.4. Trophic level

The trophic level (TL) of consumers was calculated following the equation proposed by Post (2002):

$$\mathrm{TL} = \left(\frac{\delta^{15}N_{consumer} - \delta^{15}N_{baseline}}{\mathrm{TFF}\ \delta^{15}N}\right) + 1$$

where $\delta^{15}N_{consumer}$ is the isotopic composition of the consumer, $\delta^{15}N_{baseline}$ is the isotopic composition of the size-fraction 0.7–2.7 µm considered as baseline with a trophic level of 1 and TFF $\delta^{15}N$ was fixed to 2.40 ± 0.26 ‰ (Tiselius and Fransson, 2016). TL of each size fraction was weighted to its respective biomass per station (TL_B):

$$\mathrm{TL_B} = \frac{\sum_i^n (\mathrm{TL_i} * \%\ \mathrm{Biomass_i})}{100}$$

where *I* is represented by each size fraction from 60–200 to > 2000 µm and n is the number of size-fractions.

2.5. Data treatment

The effect of size-fractions and geographical area on the SPM_{DW}, $Plankton_{DW}$, POC, PON, C/N, carbon biomass of phytoplankton, biochemical composition, energy content, isotopic composition and trophic levels were tested by means of one-way ANOVA or non-parametric Kruskal-Wallis tests after testing for normality and homogeneity of variances, followed by appropriate paired comparison tests, using the software Statistica 12. Spearman's rank order correlation tests were used to assess the significance of the correlations between our results and some environmental variables (Tedetti et al., 2023).

3. Results

3.1. Plankton dry weight, TChl*a*, POC, PON and C:N

Significant differences in SPM_{DW} were observed between the different size-fractions ($H = 23.2$, $p < 0.0001$) (Table 1). When considering all stations, the highest mean SPM_{DW} was measured in the 2.7–20 µm size-fraction (0.18 ± 0.04 mg DW L^{-1}, $n = 10$) and the lowest in the 20–60 µm fraction (0.04 ± 0.02 mg DW L^{-1}, $n = 10$). Generally, these concentrations decreased from coastal stations to offshore stations, except for St9, which exhibited the highest SPM_{DW} in the 2.7–20 µm size-fraction (Table 1). The size-fractions 0.7–2.7 and 2.7–20 µm presented the lowest values at St15. The highest SPM_{DW} in the 20–60-µm size-fraction were observed at St17, St19 and St4. TChl*a* concentrations in the > 0.7-µm fraction ranged from 0.21 (St17) to 1.54 µg L^{-1} (St9) with a mean value of 0.76 ± 0.14 µg L^{-1} ($n = 10$) (Table 1). The 60–200 and 200–500 µm zooplankton size-fractions showed the highest $Plankton_{DW}$ (Table 1). POC and PON concentrations increased with phytoplankton size with the lowest values in the 0.7–2.7 µm size-fraction (11.4 and respectively 2.1 µg C L^{-1}) and the highest ones in the 0.7–60 µm size-fraction (42.8 and respectively 6.9 µg C L^{-1}) (Table S2). The lowest POC and PON values were observed at St11 for the 0.7–2.7 µm size-fraction and at St2 for the 2.7–20 µm size-fraction (Table S2). The C:N ratios in the 0.7 to 60 µm size-fractions ranged from 5.7 at St19 to 8.5 at St9. The 0.7–2.7 µm size-fraction presented significantly lower C:N ratios than the 2.7–20-µm and the 20–60 µm size-fractions (Table S2).

3.2. Planktonic group composition

342 Different plankton groups contributed to the biomass of the different size-fractions. The size-
343 fraction 0.7–2.7 µm was on average dominated in biomass by *Synechococcus* spp. (4.6 µg C
344 L^{-1} or ~ 52%) and picoeukaryotes (4.0 µg C L^{-1} or ~ 45%) (Table S3). The size-fraction 2.7–
345 20 µm was dominated in biomass by the nanoeukaryotes (20.0 µg C L^{-1} ~ 88%) and
346 represented the highest biomass among size-fractions. The highest cumulated biomass in the
347 range 0.7–20 µm was found at St1, St9 and St19 (Table S3). POC concentration and the
348 carbon biomass of phytoplankton size-fractions between 0.7 and 20 µm showed a significant
349 linear correlation ($R^2 = 0.66$; $p = 0.018$) (Fig. S1). Carbon biomass estimated by flow
350 cytometry represented around 86% of the POC measured on filters ($y = 0.86x + 11.86$). Total
351 biomass was dominated by detritus and phytoplankton in the 60–200 and 200–500 µm size-
352 fractions (68.8 and 59.2%, respectively), which decreased with the increasing size-fractions
353 (10.5% in the > 2000-µm size-fraction) (Table S4). Copepods dominated in the zooplankton
354 biomass in the 60 to 2000 µm size-fractions (between 54.3% and 91.9%) while crustaceans
355 and gelatinous dominated the > 2000 µm size-fraction (Table S4).
356
357 **3.3. Biochemical and energy content**
358 The Mediterranean plankton sampled had for all size-fractions and stations combined, except
359 the 0.7–60-µm fraction, mean dry weight concentrations (± SE) of 222.6 ± 6.9 µg mg^{-1} DW (n
360 = 204) for proteins, 96.9 ± 6.5 µg mg^{-1} DW (n = 203) for carbohydrates, 35.1 ± 1.5 µg mg^{-1}
361 DW (n = 197) for lipids and an E_i of 7.7 ± 0.2 kJ g^{-1} DW (n = 196).
362
363 **3.3.1. Differences between plankton size-fractions**
364 Considering all stations combined, the mean concentration of proteins increased with size and
365 was significantly higher in large fractions of zooplankton (500–1000 and 1000–2000 µm)
366 than in small fractions of phytoplankton (0.7–2.7 and 2.7–20 µm). The highest mean protein
367 concentration was recorded in the 1000–2000 µm size-fraction and the lowest in the largest (>
368 2000 µm) size-fraction (Fig. 2A). The mean concentration in carbohydrates decreased with
369 size. The concentrations measured in phytoplankton (0.7–60 and 20–60 µm) were
370 significantly higher than those of the large zooplankton (1000–2000 and > 2000 µm) (Fig.
371 2B). The mean concentration in lipids was quite homogeneous between size-fractions, with
372 the highest values measured in the size-fractions 20–60 and 1000–2000 µm, and lowest in the
373 size-fractions 0.7–2.7 and > 2000 µm (Fig. 2C). Energy content showed an increasing trend
374 with size for both phyto- and zooplankton size-fractions. The highest values were measured in

the 20–60 µm and 1000-2000 µm size-fractions, respectively, and the lowest in the size-fractions 0.7–2.7 and > 2000 µm. (Fig. 2D).

3.3.2. Differences between stations

To investigate the differences between stations, the size-fractions were grouped in two fractions: the phytoplankton fraction (fractions between 0.7 and 60 µm) and the zooplankton fraction (fractions between 60 and 500 µm that were sampled at all the stations). The highest mean protein concentrations in phyto- and zooplankton fractions were recorded at St9, St11 and St15, and the lowest at St17 (Fig. 3A, B). The highest mean carbohydrate concentrations were observed at St9 for the phytoplankton (Fig. 3C). The highest mean lipid concentrations and energy values for phyto- and zooplankton were measured at St1, St2, St9 and St11, and the lowest at St3, St4 and St17 (Fig. 3E-H). Overall, greater differences appeared between stations than between size-fractions for most of these biochemical compounds (Table S5). E_{TS} ranged from 1.17 kJ m^{-3} at St3 to 6.30 kJ m^{-3} at St9 with a mean value (± SE) of 2.37 ± 0.49 kJ m^{-3} (n = 10) (Fig. 4). High E_{TS} were also observed at coastal stations St1, St4, St17 and St19. The 0.7–2.7 and 2.7–20 µm size-fractions represented the largest energetic reservoirs with mean values of 0.65 ± 0.09 kJ m^{-3} (n = 10) and 1.16 ± 0.37 kJ m^{-3} (n = 10), respectively (Fig. 4). The 200–500-µm fraction represented the largest energy reservoir for the zooplankton with a mean of 0.164 kJ m^{-3}. Although the 0.7–2.7 and 2.7–20 µm fractions had lower E_i (6.2 and 6.3 kJ g^{-1} DW, respectively) than those measured in the > 60 µm size-fractions (between 7.0 and 9.5 kJ g^{-1} DW) (Fig. 2), their dry weight was about one order of magnitude higher (Tables 1 and S2), thus enhancing their major contribution of phytoplankton to the total plankton energy amount available in the system (Fig. 4).

3.4. Stable isotope compositions ($\delta^{13}C$ and $\delta^{15}N$)

For all size fractions and stations combined, except the 0.7–60 µm fraction, the plankton $\delta^{13}C$ values ranged from –26.6 to –17.4 ‰, with a mean of –23.0 ± 0.1‰ (n = 136), whereas the $\delta^{15}N$ values ranged from –0.6 to 5.7‰, with a mean of 2.6 ± 0.1‰ (n = 136).

3.4.1. Differences between plankton size-fractions

Considering all stations combined, the mean $\delta^{13}C$ and $\delta^{15}N$ values increased with size, especially in the fractions ranging from 0.7 to 60 µm (Fig. 5, Table S6). Significantly higher mean $\delta^{13}C$ values were reported in the 20–60 µm fraction than in the 0.7–2.7 µm fraction. The mean $\delta^{15}N$ values of the size-fractions from 0.7 to 60 µm were all significantly different. Size-

fractions between 60 and 2000 µm showed slightly higher $\delta^{13}C$ values than those of smaller fractions. The highest mean $\delta^{13}C$ and $\delta^{15}N$ values were measured in the 1000 to > 2000 µm size-fractions (Fig. 5, Table S6).

3.4.2. Differences between stations

As for the biochemical composition, the size-fractions were grouped into two fractions: the phytoplankton fraction (fractions between 0.7 and 60 µm) and the zooplankton fraction (fractions between 60 and 500 µm that were sampled at all the stations). The mean $\delta^{13}C$ and $\delta^{15}N$ values followed the same spatial variations between phyto- and zooplankton fractions (Fig. 6A-D). For both phyto- and zooplankton, the highest mean $\delta^{13}C$ values were measured at St4 and St17. The highest mean $\delta^{15}N$ values were detected in phytoplankton at St4, while the lowest ones were observed at St9. In zooplankton, the highest mean $\delta^{15}N$ values were measured at St10, and the lowest ones at St9, St17, and St19 (Fig. 6A-D). Overall, in contrast to the biochemical composition, greater differences were highlighted between size-fractions than between stations for both $\delta^{13}C$ and $\delta^{15}N$ values (Table S5).

3.5. Trophic levels

For all zooplankton size-fractions (60 to > 2000 µm) and stations combined, the TL ranged from 1.5 to 3.6 with a mean of 2.2 ± 0.1 (n = 76). When considering all stations combined, mean TL significatively increased with size ($F = 5.2$, $p = 0.001$) (Fig. 7). The highest mean TL (2.6 ± 0.2, n = 10) was measured for the 1000–2000 µm size-fraction and the lowest TL (1.9 ± 0.1, n = 20) in the 60–200 µm fraction. For the 60–200, 200–500, and 500–1000 µm size-fractions, differences in mean TLs were overall significant between stations ($H = 18.7$, $p = 0.027$; $H = 18.9$, $p = 0.026$ and $H = 16.3$, $p = 0.037$, respectively) with the highest mean trophic levels by size-fraction at St10. Mean TL weighted by the plankton biomass (TL_B) had values larger than 2 at St2, St3 in northern coastal waters, and at St9, St10 and St11 in offshore waters (Fig. 8). The cumulated biomass of the zooplankton groups (60 to > 2000 µm) of the sampled stations was significantly and negatively correlated with TL_B ($R^2 = 0.61$, $p = 0.020$) (Fig. S2).

3.6. Trophic flows in the plankton food web

The Mediterranean plankton food web analysis highlighted size predation (Fig. 9, Fig. S3). For all stations combined, the 0.7–2.7 µm fraction was mainly consumed by the 60–500-µm fraction, while the consumption of the 2.7–20 µm fraction was similar between the 60–500

443 and 500–2000-µm fractions. The > 2000 µm size-fraction mainly consumed the 20–60 µm
444 size fraction (Fig. 9, Fig. S3).
445
446 ## 4. Discussion
447
448 ### 4.1. Plankton biochemical content
449 The present description of the plankton biochemical content along a north-south transect in
450 the Mediterranean Sea appears to be unique to our knowledge. The biochemistry of phyto-
451 and zooplankton has been extensively documented in many marine environments but remains
452 little observed in the Mediterranean Sea (Morris and Hopkins, 1983; Danovaro et al., 2000;
453 Yilmaz and Besiktepe, 2010; Chen et al., 2019).
454 Jónasdóttir (2019) summarizes the biochemistry of phytoplankton by a protein / carbohydrate
455 / lipid average ratio of 5 / 3 / 2 (with a range of 40–60, 17–40, and 16–26%), similar to Ríos et
456 al. (1998) who found a ratio of 4.9 / 3.2 / 1.9. In our study, the mean ratio of the size-fractions
457 between 0.7 and 60 µm was on average 5.6 / 3.6 / 0.9, therefore with relatively higher proteins
458 and lower lipids compared to previous ratios. The biochemical ratio in the > 60 µm size-
459 fractions was 6.9 / 2.0 / 1.1, reflecting higher protein and lower carbohydrate contents
460 compared to phytoplankton. The higher proportion of protein to carbohydrate is a good
461 indicator of the nitrogen availability in the environment whereas the inverse pattern may
462 reflect nitrogen-limited environments for both phyto- (Fabiano et al., 1999; Danovaro et al.,
463 2000; Yilmaz and Besiktepe, 2010; Kim et al., 2019) and zooplankton (Bhat et al., 1993).
464 Chen et al. (2019) found in spring time in the Bay of Marseille (in the same location as our
465 station St4), for the size-fraction 200–500 µm, carbohydrate concentrations (62.4 to 66.7 mg
466 g^{-1}) similar to ours, while their concentrations in lipids (98.3 to 102.8 mg g^{-1}) and proteins
467 (292.7 to 335.7 mg g^{-1}) were higher.
468 The protein and lipid concentrations were higher in zooplankton than in phytoplankton.
469 Within the zooplankton, an increase in proteins with size was observed, in agreement with
470 Guisande (2006). Most of the organisms in our samples between 60 and 2000 µm were
471 composed of copepods, and, consequently, the different fractions corresponding to different
472 life-stages of the same group (Fierro-González et al., 2023) may explain the size influence on
473 their biochemical content. The highest concentrations of carbohydrates and lipids reported in
474 the 20–60 µm size-fraction can be related to a mixed composition of microphyto- and
475 microzooplanktonic organisms, such as diatoms and metazoan eggs (Danovaro et al., 2000;
476 Chen et al., 2019). However, an underestimation of the SPM_{DW} in the 20–60 µm fraction with

respect to that in the size-fractions from 0.7 to 60 µm – due to different estimation methods (see section 2.2.2) – may explain the higher biochemical concentrations measured in the 20–60 µm fractions. Finally, the lowest protein, carbohydrate, and lipid concentrations observed in the > 2000-µm fraction were probably related to the dominance in this fraction of filter feeder organisms, such as salps and siphonophores (Bănaru et al., 2014; Hunt et al., 2017; Chen et al., 2019; Fierro-González et al., 2023).

Organic contaminants have been shown to have a strong chemical affinity for lipids or proteins (Mason et al., 1995; Wu and Wang, 2011, Frouin et al., 2013). Therefore, without considering the size of the organisms (which is also an important factor in the accumulation of contaminants in biota, in particular, phytoplankton), we can assume that the concentrations of organic contaminants in zooplankton of stations St1, St2, St9 and St11 (which contains more lipids and proteins) may be higher than those in the zooplankton of stations St3, St4 and St17 (which have less lipids and proteins). The biochemical content of the plankton size fractions can change due to variations of the composition of the plankton community and the nutrient inputs linked to the physical and chemical environment, thus affecting the entire trophodynamics of the ecosystem (Chen et al., 2019, 2021; Tedetti et al., 2023).

4.2. Plankton total energy amount (E_{TS})

The E_T decreased with size due to plankton biomass reduction with size. In our study, the E_T in SPM_{DW} were lower than previously measured in other areas (Mayzaud et al., 1989; Fabiano et al., 1999; Kim et al., 2019). This is most likely due to the lower phytoplankton biomass reported in the oligotrophic Mediterranean Sea, highlighting their low qualitative values even if spatial and seasonal variations may occur. In the eastern Mediterranean basin, the E_i measured in zooplankton by Danovaro et al., (2000) were even lower than in our study, probably related to higher oligotrophy in their study area. In the Bay of Marseille, the E_T measured at St4 were higher for us than those recorded in similar zooplankton size-fractions during the same season in 2017 by Chen et al. (2019). Plankton showed higher E_{TS} at St1, St4, St9 and St19. At these stations, where bloom conditions prevailed, trophic regimes were probably responsible for enhanced biomass (Mayot et al., 2017; Chen et al., 2019; Tedetti et al., 2023) (Table S1), which may have impacted their E_{TS}. The 0.7–2.7, 2.7–20, and 200–500-µm size-fractions represented the largest energetic reservoir in the Mediterranean phyto-, and zooplankton compartments. Our study highlights their importance as major potential sources of contaminants for their consumers.

4.3. Plankton stable isotopes ratios and composition

The fractions comprised between 0.7 and 60 µm corresponded to SPM_{DW} made up of a complex mixture of living, detrital and lithogenic material, difficult to separate (Lam et al., 2015; Tedetti et al., 2023). The main limitation of food web studies relying of stable isotope ratios is to establish an acceptable baseline, using samples mainly composed of primary producers (Harmelin-Vivien et al., 2008; Tamelander et al., 2009). In our study, pico- and nanoplankton dominated the SPM_{DW} biomass which was composed of around 86% of photosynthetic organisms, as confirmed by cytometry results (Boudriga et al., 2022). Moreover, their low C:N ratios suggest a composition dominated by living photosynthetic organisms.

Few studies have measured isotopic compositions of the smallest size-fractions of plankton (Wainright and Fry, 1994; Tamelander et al., 2009), and even fewer have separated them by size (Rau et al., 1990; Rolff, 2000; Im et al., 2015; Hunt et al., 2017; Décima, 2022). The size-fractions from 0.7 to 60 µm (without considering the 0.7–60 µm fraction) have similar $\delta^{13}C$ values but their $\delta^{15}N$ values are rather low (–23.9 ± 0.2 ‰ and 1.4 ± 0.16 ‰, respectively) compared to those measured in other oceanic basins (from –28 to –17 ‰ and from 1 to 12 ‰, respectively) (Wainright and Fry, 1994; Rolff, 2000; Tamelander et al., 2009) and in the Mediterranean Sea (from –25 to –22 ‰ and from 1 to 6 ‰, respectively) (Rau et al., 1990; Harmelin-Vivien et al., 2008; Hunt et al., 2017; Liénart et al., 2017). Several processes may explain the low $\delta^{15}N$ values of the plankton in our study: 1) in the convection areas subjected to algae blooms (such as St9), nutrients made of light isotopes are preferentially uptaken by phytoplankton (Wainright and Fry, 1994; Rolff, 2000; Tamelander et al., 2009), 2) in water with poor nutrient content, ammonium, the main nitrogen source emitted through excretion and recycling, has lower $\delta^{15}N$ values (Checkely and Miller, 1989), and 3) the high proportion of diazotrophs (atmospheric nitrogen fixer) in oligotrophic waters may lower $\delta^{15}N$ values (Pantoja et al., 2002; Montoya et al., 2002; Koppelmann et al., 2003). Within the 0.7 and 60 µm size-fractions, $\delta^{13}C$ and $\delta^{15}N$ values significantly increased with size from pico-, nano- to microplankton, similar to previous studies (Im et al., 2015; Hunt et al., 2017). Differences between primary producers can be related to differences in the isotopic composition of inorganic nitrogen sources and/or fractionation between molecules made of heavy and light isotopes during physiological processes (Ostrom and Fry, 1993). A large contribution of cyanobacteria, mainly composed of *Synechococcus* spp. may lower $\delta^{13}C$ and $\delta^{15}N$ values of SPM in the 0.7–2.7 µm size-fraction (Rau et al., 1990; Rolff, 2000; Hunt et al., 2017). These differences in the composition may also suggest predation within the 0.7–60 µm

fraction (Onodera et al., 2018; Armengol et al., 2019). However, an increase in $\delta^{15}N$ values with the size has already been observed in autotrophs (Karsh et al., 2003; Hunt et al., 2017). The group composed of size-fractions larger than 60 µm and dominated by zooplankton, mainly copepods (Fierro-González et al., 2023), presented higher $\delta^{13}C$ and $\delta^{15}N$ values than phytoplankton.

The isotopic compositions reported here for the 200–500 µm size-fractions (–22.6 ± 0.4 ‰ and 3.2 ± 0.2 ‰, for $\delta^{13}C$ and $\delta^{15}N$, respectively) were rather in the lower range of previous estimates in different oceanic basins (from –22 to –19‰ and from 2 to 8‰ for $\delta^{13}C$ and $\delta^{15}N$ values, respectively) (Fry and Quiñones, 1994; Bode et al., 2007; Yang et al., 2017). Overall, the isotopic compositions measured in the different zooplankton size-fractions were within the same range as those reported in the ultra-oligotrophic eastern Mediterranean basin (Koppelmann et al., 2009; Denda and Christiansen, 2010) and in the more productive area of the Gulf of Lion (Espinasse et al., 2014; Bănaru et al., 2014; Hunt et al., 2017).

Within the zooplankton size-fractions, $\delta^{15}N$ values increased with size, up to the 1000–2000 µm fraction, underlining an enhancement of the predation with size (Fry and Quiñones, 1994; Rolff, 2000; Bănaru et al., 2014; Espinasse et al., 2014; Hunt et al., 2017). The $\delta^{15}N$ values increased with the size-fractions, which may be due to the succession of the different life stages of copepods, coinciding with the pattern observed in their biochemical composition (Espinasse et al., 2014; Chen et al., 2019) related to metabolic changes during the lifespan (Guisande, 2006), adaptative foraging (Kozak et al., 2020), ontogenetics (Mauchline, 1998; Im et al., 2015) or all these processes combined. Fierro-González et al. (2023) reported an increase in the proportion of carnivores with size. However, in the largest size-fraction (> 2000 µm), gelatinous organisms were generally overrepresented with respect to other fractions, leading to higher $\delta^{13}C$ and lower $\delta^{15}N$ values due probably to distinct food sources from smaller fractions (Bănaru et al., 2014; Espinasse et al., 2014).

4.4. Spatial variation in plankton isotopic compositions

The highest $\delta^{15}N$ values in phytoplankton were recorded at St4, located in the Bay of Marseille, which is highly impacted by anthropogenic and terrestrial inputs. These inputs may induce, in case of declining nitrates related to intense bloom events, an increase of the $\delta^{15}N$ values (Raimbault et al., 2008; Fey et al., 2021). Moreover, the effluents of the Marseille sewage treatment plant may be ^{15}N-enriched in the inorganic nitrogen pool due to bacterial denitrification (Wainright and Fry, 1994; Cabana and Rasmussen, 1996). The high $\delta^{13}C$ values measured in phyto- and zooplankton in the Bay of Marseille (St3 and St4) and in the

579 Gulf of Gabès (St17 and St19) may be due to higher growth rates and nutrient availability in
580 these productive areas (Laws et al., 1995; Bidigare et al., 1997), as well as to inputs of
581 sedimentary organic matter in the water column during sediment resuspension events (Table
582 S1). Moreover, the low $\delta^{15}N$ values measured on the Tunisian coasts support this hypothesis
583 and may be related to seagrass detritus (Cresson et al., 2012). St9, located at the border of the
584 convective area of the Northwestern Mediterranean Sea, was characterized by a post-bloom
585 event during the campaign (Tedetti et al., 2023) and displayed the lowest $\delta^{15}N$ values in
586 phyto- and zooplanktonic organisms. The highest C:N measured at this station may suggest a
587 higher detrital organic matter content and a higher microbial production of regenerated
588 isotopically lighter ammonium compared to the other stations (Maguer et al., 2000).
589 The relatively high $\delta^{13}C$ (and $\delta^{15}N$) values measured in phyto- and zooplankton in the Bay of
590 Marseille and the Gulf of Gabès may also be related to various inputs (sediment resuspension,
591 effluents, etc.), and be the sign of higher levels of contaminants which could derive from the
592 same sources. To support this hypothesis, higher trace metal concentrations have been
593 reported in these coastal stations compared to other MERITE-HIPPOCAMPE stations
594 (Chifflet et al., 2023).
595
596 **4.5. Trophic levels and food web implications**
597 The TLs determined in this study, ranging from 1.5 to 3.6, increased with size and spread out
598 over 2 TLs. TLs lower than 2 may be related to a mixture of primary producers and
599 consumers mainly found at some stations in the 60–200 µm size-fraction, related to clogging
600 of the sampling device caused by phytoplankton. Further improvements in sampling methods
601 by using larger mesh-size nets for zooplankton size-fractions collection may avoid potential
602 clogging during bloom events and the presence of phytoplankton within the 60–200 µm size-
603 fraction.
604 When biomass is averaged to the TL of zooplankton (TL_B), higher values are obtained at the
605 coastal (St2, and St3), and offshore (St9, St10, and St11) stations. High adaptability in food
606 habits of zooplankton is well known and omnivory seems to be the most common trophic
607 pathway (Fierro-González et al., 2023). Higher TLs are generally reached in microbial food
608 webs, often observed in oligotrophic regimes (Søreide et al., 2006; Kürten et al., 2013). St10
609 and St11 contained carnivorous plankton, such as chaetognaths which may explain the higher
610 TLs of the zooplankton community observed in these areas (Fierro-González et al., 2023). It
611 has been suggested that the TFF between phytoplankton and protozoans is equal to 0,
612 contributing to an underestimation of the number of TLs in planktonic food webs (Gutiérrez-

Rodríguez et al., 2014). However, in this work, we suggest that the higher TLs of plankton were probably related to the microbial food web.

Coastal stations (St1, St4, St15, St17 and St19) were characterized by lower TL_B. The lower TL of plankton in productive systems is classic in herbivore food webs, dominated by larger phytoplankton organisms readily available to zooplankton (Sommer et al., 2002; Fileman et al., 2007). Food chain length decreases in productive ecosystems due to an adaptive foraging of consumers which selects the most abundant low TL resources (Kondoh and Ninomiya, 2009). Detritus and phytoplankton were dominant in these stations in the 60–200 µm size-fraction contributing to lowering TL_B values (Fierro-González et al., 2023).

In addition, the zooplankton biomass was related to the trophic pathways. A negative relationship between the TL_B and the zooplankton biomass was observed during this study. Higher biomasses of zooplankton have been measured at coastal stations relative to offshore areas in relation to their primary production (Champalbert, 1996). Where TLs were high (St9, St10 and St11), large size fractions (500–1000 and 1000–2000 µm) were also well represented, accounting for 27 to 54% of the total zooplankton biomass. Espinasse et al. (2014) have already highlighted the overrepresentation of large plankton organisms in moderately productive areas, while Décima (2022) have reported an inverse relationship between food chain length and productivity in zooplankton. Although located in the offshore area, St9 was characterized by a still productive post-bloom situation (Tedetti et al., 2023) with high TL_B. Usually, during post-bloom, diatoms give way to inedible algae not consumed by zooplankton organisms and the source of organic matter is obtained through the cell lysis, fuelling microbial loop and enhancing food steps (Sommer et al., 2002). High C:N ratios observed at St9 may indicate heterotrophy within the 0.7–60 µm fractions (Harmelin-Vivien et al., 2008). The post-bloom situation may induce a decrease of the resources and thus mesoplankton preying on microplankton (Levinsen et al., 2000; Basedow et al., 2016). Hence, the results reported here highlight different trophodynamic scenarios in the Mediterranean plankton food webs and their control on planktonic biomasses, as hypothesized by Fry and Quiñones (1994).

Contrasting carbon fluxes can impact contaminant transfer. The ability of each contaminant to bioaccumulate can lead to different scenarios. In low-productive ecosystems, organic matter fluxes go through more trophic steps, which can favor a higher transfer of contaminants that will bioaccumulate such as methylmercury, PCBs or Cd (Tiano et al., 2014; Schartup et al., 2018; Chouvelon et al., 2019). Conversely, in productive ecosystems, direct access to organic matter sources and reduced food steps favors higher transfer of contaminants with little or no

capacity to bioaccumulate, such as the numerous trace elements Co, Ni, Cu, Ag, Pb, and Zn (Chouvelon et al., 2019).

4.6. Plankton food web flows

The difference in stable isotope composition between phytoplankton size-fractions made them relevant candidates for mixing model analysis of their relative contributions to zooplankton biomass (Phillips et al., 2014; Hunt et al., 2017). Overall, the contribution of the 0.7–2.7-µm size-fraction to the diet of the 60–500 µm size fraction underlines the role of the microzooplankton (60–200 µm) and of the small mesozooplankton (200–500 µm) in the transfer of organic matter from the baseline to higher trophic level consumers. The picoplankton size fraction was mainly composed of *Synechococcus* spp., the most abundant phytoplankton organism in the Mediterranean Sea that sustains primary production (Boudriga et al., 2022). In fact, during the MERITE-HIPPOCAMPE campaign, picoplankton accounted for, on average, 27% of the total biomass of phytoplankton.

Classically, we consider that nanoflagellates and microzooplankton (from 2 to 200 µm size-fractions) may represent intermediate food steps (Ryther, 1969; Calbet and Landry, 1999) ensuring the link between the 0.7–2.7 µm fraction and mesozooplankton (200–2000 µm) (Sommer et al., 2000). The 60 to 500 µm size-fractions were constituted of a large percentage of phytoplankton and detritus that would have contributed to lowering their stable isotope ratios. This may have consequences with regard to the mixing model results and may explain the high percentage of picoplankton estimated in the diet of 60–500 µm size-fraction. However, in agreement with our results, and despite their small size, recent studies demonstrated that small copepods may feed on picoplankton (Motwani and Gorokhova, 2013; Im et al., 2015; Major et al., 2017).

Primary producers were also dominant in the 2.7–20 µm fractions, representing 69% of the phytoplanktonic biomass and about half of the total food supply to both the 60–500 and the 500–2000 µm size-fractions. Nanoplankton was mainly composed of nanoeukaryotes and its contribution to the planktonic food web seems essential, in agreement with the results of Hunt et al. (2017). Finally, the 20–60 µm fraction has low biomass and represents an important contribution only to the diet of the > 2000 µm size-fractions. TFFs for plankton should be experimentally determined and a higher number of replicates should be analyzed to improve model results and to reduce their variability.

Differences in contaminant accumulation have been reported in phytoplankton size-fractions. Trace metals reflected, for each element, contrasted accumulation patterns between small and

large phytoplankton fractions (Chifflet et al., 2023). Higher methylmercury concentrations were reported during a picoplanktonic bloom, probably due to a higher surface to volume ratio, favoring uptake (Heimbürger et al., 2010). In addition, for PCBs, a higher accumulation was observed in smaller cells (Axelman et al., 1997). The different carbon size-fractions of food sources can thus influence the transfer of contaminants and concentrations in zooplankton consumers.

5. Conclusions

During the MERITE-HIPPOCAMPE campaign, plankton size-fractions revealed contrasted biochemical and isotopic compositions related to their size, composition and location. Carbohydrate concentrations were the highest in phytoplankton (between 0.7 and 60 µm size-fractions) with respect to zooplankton (> 60 µm size-fractions), which displayed high protein and lipid contents increasing with size. The affinity of proteins and lipids for contaminants makes zooplankton more sensitive to their accumulation (regardless of the size of organisms). Due to the high amount of energy contained in their biomass, the pico- and nanoplankton represents a major food resource in Mediterranean ecosystems fueling the zooplankton food webs and an essential pathway for contaminants due to the combination of small size and high energetic content. In the zooplankton community, the 200–500 µm size-fraction, dominated by copepods, showed the highest energy amount, which explains their role as essential food resource for many planktivorous fishes. Spatial variations of isotopic compositions of plankton size-fractions were also observed, revealing different carbon sources between the coast and the offshore areas, and between the Bay of Gabès (southern coast) and the Bay of Toulon (northern coast), and resulting in a different exposure to contaminants. Trophic levels revealed increasing predation with size, which can result in the biomagnification of contaminants. Trophic pathways in planktonic food webs displayed spatial variations influenced by the availability of phytoplankton resources. Higher predation occurred in low productive areas where the zooplankton community reached the highest mean trophic levels, increasing the potential exposure of planktonic food webs to contaminants. Our findings on the spatial variations of the biomass, biochemical composition, and the role of the different plankton size-fractions in the food web, as well as the different flows of organic matter in the pelagic food webs, are an essential step for the comprehension of the transfer of contaminants in the Mediterranean pelagic food webs.

Author contribution statement

Conception and design of study: DB, MT, FC, MP,

Acquisition of data: JATO, MeTe, LG, PF, BL, GG, IB, MB, AZ, MT, SC

Analysis and/or interpretation of data: JATO, DB, MT, TG, CC, SC

Drafting of the manuscript: JATO, DB, MT

Revising/editing of the manuscript: JATO, DB, MT, FC, BL

Project administration and funding acquisition: DB, MT, FC, MP

Acknowledgements

The authors wish to thank the crew of the R/V *Antea* and the various platforms of the Mediterranean Institute of Oceanography having contributed to the data acquisition: Plateforme Analytique de Chimie des Environnements Marins (PACEM) for the POC/PON measurements, Plateforme Régionale de Cytométrie pour la Microbiologie (PRECYM) for cytometric analyses, Microscopie et Imagerie numérique (MIM) for identification expertise and the Service Atmosphère-Mer (SAM) for the technical and operational tasks. The authors thank the LIENSs joint research unit (CNRS - La Rochelle University) for the measurement of $\delta^{13}C$ and $\delta^{15}N$ values. The MERITE-HIPPOCAMPE project has been funded by the cross-disciplinary *Pollution & Contaminants* axis of the CNRS-INSU MISTRALS program (joint action of the MERMEX-MERITE and CHARMEX subprograms) and received support from the IRD French-Tunisian International Joint Laboratory (LMI) COSYS-Med. We are grateful for the additional funding received from IFREMER, the MIO Action Sud and Transverse Axis programs (CONTAM Transverse Axis), and from the IRD Ocean Department. This study received funding by the CONTAMPUMP project (ANR JCJC #19-CE34-0001-01). Finally, we warmly thank three anonymous Reviewers for their very relevant and useful comments and corrections on the manuscript, as well as Michael Paul for the English corrections.

Supplementary information

Supplementary material related to this article is available online at: xxx

References

Alekseenko, E., Thouvenin, B., Tronczyński, J., Carlotti, F., Garreau, P., Tixier, C., Baklouti, M., 2018. Modeling of PCB trophic transfer in the Gulf of Lions; 3D coupled model

748 application. Marine Pollution Bulletin 128, 140–155.
749 https://doi.org/10.1016/j.marpolbul.2018.01.008
750 Armengol, L., Calbet, A., Franchy, G., Rodríguez-Santos, A., Hernández-León, S., 2019.
751 Planktonic food web structure and trophic transfer efficiency along a productivity
752 gradient in the tropical and subtropical Atlantic Ocean. Scientific Reports 9, 2044.
753 https://doi.org/10.1038/s41598-019-38507-9
754 Axelman, J., Broman, D., Näf, C., 1997. Field Measurements of PCB Partitioning between
755 Water and Planktonic Organisms: Influence of Growth, Particle Size, and
756 Solute−Solvent Interactions. Environmental Science & Technology 31, 665–669.
757 https://doi.org/10.1021/es960088+
758 Bănaru, D., Carlotti, F., Barani, A., Grégori, G., Neffati, N., Harmelin-Vivien, M., 2014.
759 Seasonal variation of stable isotope ratios of size-fractionated zooplankton in the Bay of
760 Marseille (NW Mediterranean Sea). Journal of Plankton Research 36, 145–156.
761 https://doi.org/10.1093/plankt/fbt083
762 Bănaru, D., Diaz, F., Verley, P., Campbell, R., Navarro, J., Yohia, C., Oliveros-Ramos, R.,
763 Mellon-Duval, C., Shin, Y.-J., 2019. Implementation of an end-to-end model of the Gulf
764 of Lions ecosystem (NW Mediterranean Sea). I. Parameterization, calibration and
765 evaluation. Ecological Modelling 401, 1–19.
766 https://doi.org/10.1016/j.ecolmodel.2019.03.005
767 Bănaru, D., Mellon-Duval, C., Roos, D., Bigot, J.-L., Souplet, A., Jadaud, A., Beaubrun, P.,
768 Fromentin, J.-M., 2013. Trophic structure in the Gulf of Lions marine ecosystem (north-
769 western Mediterranean Sea) and fishing impacts. Journal of Marine Systems 111–112,
770 45–68. https://doi.org/10.1016/j.jmarsys.2012.09.010
771 Banse, K., Mosher, S., 1980. Adult Body Mass and Annual Production/Biomass Relationships
772 of Field Populations. Ecological Monographs 50, 355–379.
773 https://doi.org/10.2307/2937256
774 Basedow, S.L., de Silva, N.A.L., Bode, A., van Beusekorn, J., 2016. Trophic positions of
775 mesozooplankton across the North Atlantic: estimates derived from biovolume spectrum
776 theories and stable isotope analyses. Journal of Plankton Research 38, 1364–1378.
777 https://doi.org/10.1093/plankt/fbw070
778 Bhat, K.L., Rayadurga, S., Ansari, Z.A., 1993. Biochemical composition of zooplankton from
779 the northern Arabian Sea. Pakistan Journal of Marine Sciences2, 17-22.
780 Bidigare, R.R., Fluegge, A., Freeman, K.H., Hanson, K.L., Hayes, J.M., Hollander, D.,
781 Jasper, J.P., King, L.L., Laws, E.A., Milder, J., Millero, F.J., Pancost, R., Popp, B.N.,

Steinberg, P.A., Wakeham, S.G., 1997. Consistent fractionation of 13C in nature and in the laboratory: Growth-rate effects in some haptophyte algae. Global Biogeochemical Cycles 11, 279–292. https://doi.org/10.1029/96GB03939

Bishop, J.K.B., Edmond, J.M., Ketten, D.R., Bacon, M.P., Silker, W.B., 1977. The chemistry, biology, and vertical flux of particulate matter from the upper 400 m of the equatorial Atlantic Ocean. Deep Sea Research 24, 511–548. https://doi.org/10.1016/0146-6291(77)90526-4

Bishop, J.K.B., Lam, P.J., Wood, T.J., 2012. Getting good particles: Accurate sampling of particles by large volume in-situ filtration: Getting good particles. Limnology and Oceanography: Methods 10, 681–710. https://doi.org/10.4319/lom.2012.10.681

Bligh, E.G., Dyer, W.J., 1959. A rapid method of total lipid extraction and purification. Canadian Journal of Biochemistry and Physiology 37, 911–917. https://doi.org/10.1139/o59-099

Bode, A., Alvarez-Ossorio, M.T., Cunha, M.E., Garrido, S., Peleteiro, J.B., Porteiro, C., Valdés, L., Varela, M., 2007. Stable nitrogen isotope studies of the pelagic food web on the Atlantic shelf of the Iberian Peninsula. Progress in Oceanography, 74, 115–131. https://doi.org/10.1016/j.pocean.2007.04.005

Boudriga, I., Thyssen, M., Zouari, A., Garcia, N., Tedetti, M., Bel Hassen, M., 2022. Ultraphytoplankton community structure in subsurface waters along a North-South Mediterranean transect. Marine Pollution Bulletin 182, 113977. https://doi.org/10.1016/j.marpolbul.2022.113977

Brown, J.H., Gillooly, J.F., Allen, A.P., Savage, V.M., West, G.B., 2004. Toward a Metabolic Theory of Ecology. Ecology 85, 1771–1789. https://doi.org/10.1890/03-9000

Cabana, G., Rasmussen, J.B., 1994. Modelling food chain structure and contaminant bioaccumulation using stable nitrogen isotopes. Nature 372, 255–257. https://doi.org/10.1038/372255a0

Cabana, G., Rasmussen, J.B., 1996. Comparison of aquatic food chains using nitrogen isotopes. Proceedings of the National Academy of Sciences 93, 10844–10847. https://doi.org/10.1073/pnas.93.20.10844

Calbet, A., Landry, M.R., 1999. Mesozooplankton influences on the microbial food web: Direct and indirect trophic interactions in the oligotrophic open ocean. Limnology and Oceanography 44, 1370–1380. https://doi.org/10.4319/lo.1999.44.6.1370

Carlotti, F., Thibault-Botha, D., Nowaczyk, A., Lefèvre, D., 2008. Zooplankton community structure, biomass and role in carbon fluxes during the second half of a phytoplankton

bloom in the eastern sector of the Kerguelen Shelf (January–February 2005). Deep Sea Research Part II: Topical Studies in Oceanography, 55, 720–733. https://doi.org/10.1016/j.dsr2.2007.12.010

Champalbert, G., 1996. Characteristics of zooplankton standing stock and communities in the western Mediterranean Sea: relations to hydrology. Scientia Marina 60, 97–113.

Checkley, D.M., Miller, C.A., 1989. Nitrogen isotope fractionation by oceanic zooplankton. Deep Sea Research Part A. Oceanographic Research Papers 36, 1449–1456. https://doi.org/10.1016/0198-0149(89)90050-2

Chen, C.-T., Bănaru, D., Carlotti, F., Faucheux, M., Harmelin-Vivien, M., 2019. Seasonal variation in biochemical and energy content of size-fractionated zooplankton in the Bay of Marseille (North-Western Mediterranean Sea). Journal of Marine Systems 199, 103223. https://doi.org/10.1016/j.jmarsys.2019.103223

Chen, C.-T., Carlotti, F., Harmelin-Vivien, M., Guilloux, L., Bănaru, D., 2021. Temporal variation in prey selection by adult European sardine (Sardina pilchardus) in the NW Mediterranean Sea. Progress in Oceanography 196, 102617. https://doi.org/10.1016/j.pocean.2021.102617

Chen, C.-T., Carlotti, F., Harmelin-Vivien, M., Lebreton, B., Guillou, G., Vassallo, L., Le Bihan, M., Bănaru, D., 2022. Diet and trophic interactions of Mediterranean planktivorous fishes. Marine Biology 169, 119. https://doi.org/10.1007/s00227-022-04103-1

Chifflet, S., Briant, N., Tesán-Onrubia, J.A., Zaaboub, N., Amri, S., Radakovitch, O., Bănaru, D., Tedetti, M., 2023. Distribution and accumulation of trace metal in the planktonic food web of the Mediterranean Sea (MERITE-HIPPOCAMPE campaign). Marine Pollution Bulletin 186, 114384. https://doi.org/10.1016/j.marpolbul.2022.114384.

Chouvelon, T., Strady, E., Harmelin-Vivien, M., Radakovitch, O., Brach-Papa, C., Crochet, S., Knoery, J., Rozuel, E., Thomas, B., Tronczynski, J., Chiffoleau, J.-F., 2019. Patterns of trace metal bioaccumulation and trophic transfer in a phytoplankton-zooplankton-small pelagic fish marine food web. Marine Pollution Bulletin 146, 1013–1030. https://doi.org/10.1016/j.marpolbul.2019.07.047

Cohen, J.E., Pimm, S.L., Yodzis, P., Saldana, J., 1993. Body Sizes of Animal Predators and Animal Prey in Food Webs. The Journal of Animal Ecology 62, 67. https://doi.org/10.2307/5483

Cossa, D., Knoery, J., Bănaru, D., Harmelin-Vivien, M., Sonke, J.E., Hedgecock, I.M., Bravo, A.G., Rosati, G., Canu, D., Horvat, M., Sprovieri, F., Pirrone, N., Heimbürger-Boavida,

L.-E., 2022. Mediterranean Mercury Assessment 2022: An Updated Budget, Health Consequences, and Research Perspectives. Environmental Science & Technology 56, 3840–3862. https://doi.org/10.1021/acs.est.1c03044

Cresson, P., Ruitton, S., Fontaine, M.-F., Harmelin-Vivien, M., 2012. Spatio-temporal variation of suspended and sedimentary organic matter quality in the Bay of Marseilles (NW Mediterranean) assessed by biochemical and isotopic analyses. Marine Pollution Bulletin 64, 1112–1121. https://doi.org/10.1016/j.marpolbul.2012.04.003

Cresson, P., Chouvelon, T., Bustamante, P., Bănaru, D., Baudrier, J., Le Loc'h, F., Mauffret, A., Mialet, B., Spitz, J., Wessel, N., Briand, M.J., Denamiel, M., Doray, M., Guillou, G., Jadaud, A., Lazard, C., Prieur, S., Rouquette, M., Saraux, C., Serre, S., Timmerman, C.-A., Verin, Y., Harmelin-Vivien, M., 2020. Primary production and depth drive different trophic structure and functioning of fish assemblages in French marine ecosystems. Progress in Oceanography 186, 102343. https://doi.org/10.1016/j.pocean.2020.102343

Danovaro, R., Dell'Anno, A., Pusceddu, A., Marrale, D., Della Croce, N., Fabiano, M., Tselepides, A., 2000. Biochemical composition of pico-, nano- and micro-particulate organic matter and bacterioplankton biomass in the oligotrophic Cretan Sea (NE Mediterranean). Progress in Oceanography 46, 279–310. https://doi.org/10.1016/S0079-6611(00)00023-9

Décima, M., 2022. Zooplankton trophic structure and ecosystem productivity. Marine Ecology Progress Series 692, 23–42. https://doi.org/10.3354/meps14077

Denda, A., Christiansen, B., 2010. Zooplankton at a seamount in the eastern Mediterranean: distribution and trophic interactions. Journal of the Marine Biological Association of the United Kingdom 91, 33–49. https://doi.org/10.1017/S0025315410001153

DuBois, Michel., Gilles, K.A., Hamilton, J.K., Rebers, P.A., Smith, Fred., 1956. Colorimetric Method for Determination of Sugars and Related Substances. Analytical Chemistry 28, 350–356. https://doi.org/10.1021/ac60111a017

Durrieu de Madron, X., Guieu, C., Sempéré, R., Conan, P., Cossa, D., D'Ortenzio, F., Estournel, C., Gazeau, F., Rabouille, C., Stemmann, L., Bonnet, S., Diaz, F., Koubbi, P., Radakovitch, O., Babin, M., Baklouti, M., Bancon-Montigny, C., Belviso, S., Bensoussan, N., Bonsang, B., Bouloubassi, I., Brunet, C., Cadiou, J.-F., Carlotti, F., Chami, M., Charmasson, S., Charrière, B., Dachs, J., Doxaran, D., Dutay, J.-C., Elbaz-Poulichet, F., Eléaume, M., Eyrolles, F., Fernandez, C., Fowler, S., Francour, P., Gaertner, J.C., Galzin, R., Gasparini, S., Ghiglione, J.-F., Gonzalez, J.-L., Goyet, C., Guidi, L., Guizien, K., Heimbürger, L.-E., Jacquet, S.H.M., Jeffrey, W.H., Joux, F., Le

884 Hir, P., Leblanc, K., Lefèvre, D., Lejeusne, C., Lemé, R., Loÿe-Pilot, M.-D., Mallet, M.,
885 Méjanelle, L., Mélin, F., Mellon, C., Mérigot, B., Merle, P.-L., Migon, C., Miller, W.L.,
886 Mortier, L., Mostajir, B., Mousseau, L., Moutin, T., Para, J., Pérez, T., Petrenko, A.,
887 Poggiale, J.-C., Prieur, L., Pujo-Pay, M., Pulido-Villena, Raimbault, P., Rees, A.P.,
888 Ridame, C., Rontani, J.-F., Ruiz Pino, D., Sicre, M.A., Taillandier, V., Tamburini, C.,
889 Tanaka, T., Taupier-Letage, I., Tedetti, M., Testor, P., Thébault, H., Thouvenin, B.,
890 Touratier, F., Tronczynski, J., Ulses, C., Van Wambeke, F., Vantrepotte, V., Vaz, S.,
891 Verney, R., 2011. Marine ecosystems' responses to climatic and anthropogenic forcings
892 in the Mediterranean. Progress in Oceanography 91, 97–166.
893 https://doi.org/10.1016/j.pocean.2011.02.003
894 Espinasse, B., Harmelin-Vivien, M., Tiano, M., Guilloux, L., Carlotti, F., 2014. Patterns of
895 variations in C and N stable isotope ratios in size-fractionated zooplankton in the Gulf of
896 Lion, NW Mediterranean Sea. Journal of Plankton Research 36, 1204–1215.
897 https://doi.org/10.1093/plankt/fbu043
898 Fabiano, M., Danovaro, R., Povero, P., 1999. Vertical Distribution and Biochemical
899 Composition of Pico- and Microparticulate Organic Matter in the Ross Sea (Antarctica),
900 in: Spezie, G., Manzella, G.M.R. (Eds.), Oceanography of the Ross Sea Antarctica.
901 Springer Milan, Milano, pp. 233–246. https://doi.org/10.1007/978-88-470-2250-8_16
902 Fan, C.-W., Reinfelder, J.R., 2003. Phenanthrene Accumulation Kinetics in Marine Diatoms.
903 Environmental Science & Technology 37, 3405–3412. https://doi.org/10.1021/es026367g
904 Fey, P., Parravicini, V., Bănaru, D., Dierking, J., Galzin, R., Lebreton, B., Meziane, T.,
905 Polunin, N.V.C., Zubia, M., Letourneur, Y., 2021. Multi-trophic markers illuminate the
906 understanding of the functioning of a remote, low coral cover Marquesan coral reef food
907 web. Scientific Reports 11, 20950. https://doi.org/10.1038/s41598-021-00348-w
908 Fierro-González, P., Pagano, M., Guilloux, L., Makhlouf, N., Tedetti, M., Carlotti, F., 2023.
909 Zooplankton biomass, size structure, and associated metabolic fluxes with focus on its
910 roles at the chlorophyll maximum layer during the plankton-contaminant MERITE-
911 HIPPOCAMPE cruise. Submitted to this special issue.
912 Fileman, E., Smith, T., Harris, R., 2007. Grazing by Calanus helgolandicus and Para-
913 Pseudocalanus spp. on phytoplankton and protozooplankton during the spring bloom in
914 the Celtic Sea. Journal of Experimental Marine Biology and Ecology 348, 70–84.
915 https://doi.org/10.1016/j.jembe.2007.04.003
916 Frouin, H., Dangerfield, N., Macdonald, R.W., Galbraith, M., Crewe, N., Shaw, P., Mackas,
917 D., Ross, P.S., 2013. Partitioning and bioaccumulation of PCBs and PBDEs in marine

plankton from the Strait of Georgia, British Columbia, Canada. Progress in Oceanography, Strait of Georgia Ecosystem Research Initiative (ERI) 115, 65–75. https://doi.org/10.1016/j.pocean.2013.05.023

Fry, B., Quiñones, R.B., 1994. Biomass spectra and stable isotope indicators of trophic level in zooplankton of the northwest Atlantic. Marine Ecology Progress Series 112, 201–204.

Guisande, C., 2006. Biochemical fingerprints in zooplankton. Limnetica 25, 369–376.

Gutiérrez-Rodríguez, A., Décima, M., Popp, B.N., Landry, M.R., 2014. Isotopic invisibility of protozoan trophic steps in marine food webs. Limnology and Oceanography 59, 1590–1598. https://doi.org/10.4319/lo.2014.59.5.1590

Harmelin-Vivien, M., Bănaru, D., Dromard, C.R., Ourgaud, M., Carlotti, F., 2019. Biochemical composition and energy content of size-fractionated zooplankton east of the Kerguelen Islands. Polar Biology 42, 603–617. https://doi.org/10.1007/s00300-019-02458-8

Harmelin-Vivien, M., Loizeau, V., Mellon, C., Beker, B., Arlhac, D., Bodiguel, X., Ferraton, F., Hermand, R., Philippon, X., Salen-Picard, C., 2008. Comparison of C and N stable isotope ratios between surface particulate organic matter and microphytoplankton in the Gulf of Lions (NW Mediterranean). Continental Shelf Research, 28, 1911–1919. https://doi.org/10.1016/j.csr.2008.03.002

Heimbürger, L.-E., Cossa, D., Marty, J.-C., Migon, C., Averty, B., Dufour, A., Ras, J., 2010. Methyl mercury distributions in relation to the presence of nano- and picophytoplankton in an oceanic water column (Ligurian Sea, North-western Mediterranean). Geochimica et Cosmochimica Acta 74, 5549–5559. https://doi.org/10.1016/j.gca.2010.06.036

Hirst, A.G., Kiørboe, T., 2002. Mortality of marine planktonic copepods: global rates and patterns. Marine Ecology Progress Series 230, 195–209. https://doi.org/10.3354/meps230195

Hunt, B.P.V., Carlotti, F., Donoso, K., Pagano, M., D'Ortenzio, F., Taillandier, V., Conan, P., 2017. Trophic pathways of phytoplankton size classes through the zooplankton food web over the spring transition period in the north-west Mediterranean Sea. Journal of Geophysical Research: Oceans 122, 6309–6324. https://doi.org/10.1002/2016JC012658

Im, D.-H., Wi, J.H., Suh, H.-L., 2015. Evidence for ontogenetic feeding strategies in four calanoid copepods in the East Sea (Japan Sea) in summer, revealed by stable isotope analysis. Ocean Science Journal 50, 481–490. https://doi.org/10.1007/s12601-015-0044-y

Jónasdóttir, S.H., 2019. Fatty Acid Profiles and Production in Marine Phytoplankton. Marine Drugs 17, 151. https://doi.org/10.3390/md17030151

952 Karsh, K.L., Trull, T.W., Lourey, M.J., Sigman, D.M., 2003. Relationship of nitrogen isotope
953 fractionation to phytoplankton size and iron availability during the Southern Ocean Iron
954 RElease Experiment (SOIREE). Limnology and Oceanography 48, 1058–1068.
955 https://doi.org/10.4319/lo.2003.48.3.1058
956 Khammeri, Y., Bellaaj-Zouari, A., Hamza, A., Medhioub, W., Sahli, E., Akrout, F., Barraj,
957 N., Ben Kacem, M.Y., Bel Hassen, M., 2020. Ultraphytoplankton community
958 composition in Southwestern and Eastern Mediterranean Basin: Relationships to water
959 mass properties and nutrients. Journal of Sea Research 158, 101875.
960 https://doi.org/10.1016/j.seares.2020.101875
961 Khammeri, Y., Hamza, I.S., Zouari, A.B., Hamza, A., Sahli, E., Akrout, F., Ben Kacem,
962 M.Y., Messaoudi, S., Hassen, M.B., 2018. Atmospheric bulk deposition of dissolved
963 nitrogen, phosphorus and silicate in the Gulf of Gabès (South Ionian Basin); implications
964 for marine heterotrophic prokaryotes and ultraphytoplankton. Continental Shelf Research
965 159, 1–11. https://doi.org/10.1016/j.csr.2018.03.003
966 Kim, Y., Lee, Jang Han, Kang, J.J., Lee, Jae Hyung, Lee, H.W., Kang, C.K., Lee, S.H., 2019.
967 River discharge effects on the contribution of small-sized phytoplankton to the total
968 biochemical composition of POM in the Gwangyang Bay, Korea. Estuarine, Coastal and
969 Shelf Science 226, 106293. https://doi.org/10.1016/j.ecss.2019.106293
970 Kondoh, M., Ninomiya, K., 2009. Food-chain length and adaptive foraging. Proceedings of
971 the Royal Society B: Biological Sciences 276, 3113–3121.
972 https://doi.org/10.1098/rspb.2009.0482
973 Koppelmann, R., Weikert, H., Lahajnar, N., 2003. Vertical distribution of mesozooplankton
974 and its δ15N signature at a deep-sea site in the Levantine Sea (eastern Mediterranean) in
975 April 1999. Journal of Geophysical Research: Oceans 108.
976 https://doi.org/10.1029/2002JC001351
977 Koppelmann, R., Böttger-Schnack, R., Möbius, J., Weikert, H., 2009. Trophic relationships of
978 zooplankton in the eastern Mediterranean based on stable isotope measurements. Journal
979 of Plankton Research 31, 669–686. https://doi.org/10.1093/plankt/fbp013
980 Kozak, E.R., Franco-Gordo, C., Godínez-Domínguez, E., Suárez-Morales, E., Ambriz-
981 Arreola, I., 2020. Seasonal variability of stable isotope values and niche size in tropical
982 calanoid copepods and zooplankton size fractions. Marine Biology 167, 37.
983 https://doi.org/10.1007/s00227-020-3653-7
984 Krasakopoulou, E., Karageorgis, A.P., 2005. Spatial and temporal distribution patterns of
985 suspended particulate matter and particulate organic carbon in the Saronikos Gulf

(eastern Mediterranean, Greece). Geo-Marine Letters 25, 343–359. https://doi.org/10.1007/s00367-005-0007-x

Kürten, B., Painting, S.J., Struck, U., Polunin, N.V.C., Middelburg, J.J., 2013. Tracking seasonal changes in North Sea zooplankton trophic dynamics using stable isotopes. Biogeochemistry 113, 167–187. https://doi.org/10.1007/s10533-011-9630-y

Lam, P.J., Ohnemus, D.C., Auro, M.E., 2015. Size-fractionated major particle composition and concentrations from the US GEOTRACES North Atlantic Zonal Transect. Deep Sea Research Part II: Topical Studies in Oceanography, 116, 303–320. https://doi.org/10.1016/j.dsr2.2014.11.020

Laws, E.A., Popp, B.N., Bidigare, R.R., Kennicutt, M.C., Macko, S.A., 1995. Dependence of phytoplankton carbon isotopic composition on growth rate and [CO2]aq: Theoretical considerations and experimental results. Geochimica et Cosmochimica Acta 59, 1131–1138. https://doi.org/10.1016/0016-7037(95)00030-4

Leblanc, K., Quéguiner, B., Diaz, F., Cornet, V., Michel-Rodriguez, M., Durrieu de Madron, X., Bowler, C., Malviya, S., Thyssen, M., Grégori, G., Rembauville, M., Grosso, O., Poulain, J., de Vargas, C., Pujo-Pay, M., Conan, P., 2018. Nanoplanktonic diatoms are globally overlooked but play a role in spring blooms and carbon export. Nature Communications 9, 953. https://doi.org/10.1038/s41467-018-03376-9

Levinsen, H., Turner, J.T., Nielsen, T.G., Hansen, B.W., 2000. On the trophic coupling between protists and copepods in arctic marine ecosystems. Marine Ecology Progress Series 204, 65–77. https://doi.org/10.3354/meps204065

Liénart, C., Savoye, N., Bozec, Y., Breton, E., Conan, P., David, V., Feunteun, E., Grangeré, K., Kerhervé, P., Lebreton, B., Lefebvre, S., L'Helguen, S., Mousseau, L., Raimbault, P., Richard, P., Riera, P., Sauriau, P.-G., Schaal, G., Aubert, F., Aubin, S., Bichon, S., Boinet, C., Bourasseau, L., Bréret, M., Caparros, J., Cariou, T., Charlier, K., Claquin, P., Cornille, V., Corre, A.-M., Costes, L., Crispi, O., Crouvoisier, M., Czamanski, M., Del Amo, Y., Derriennic, H., Dindinaud, F., Durozier, M., Hanquiez, V., Nowaczyk, A., Devesa, J., Ferreira, S., Fornier, M., Garcia, F., Garcia, N., Geslin, S., Grossteffan, E., Gueux, A., Guillaudeau, J., Guillou, G., Joly, O., Lachaussée, N., Lafont, M., Lamoureux, J., Lecuyer, E., Lehodey, J.-P., Lemeille, D., Leroux, C., Macé, E., Maria, E., Pineau, P., Petit, F., Pujo-Pay, M., Rimelin-Maury, P., Sultan, E., 2017. Dynamics of particulate organic matter composition in coastal systems: A spatio-temporal study at multi-systems scale. Progress in Oceanography 156, 221–239. https://doi.org/10.1016/j.pocean.2017.03.001

Liénart, C., Savoye, N., David, V., Ramond, P., Rodriguez Tress, P., Hanquiez, V., Marieu, V., Aubert, F., Aubin, S., Bichon, S., Boinet, C., Bourasseau, L., Bozec, Y., Bréret, M., Breton, E., Caparros, J., Cariou, T., Claquin, P., Conan, P., Corre, A.-M., Costes, L., Crouvoisier, M., Del Amo, Y., Derriennic, H., Dindinaud, F., Duran, R., Durozier, M., Devesa, J., Ferreira, S., Feunteun, E., Garcia, N., Geslin, S., Grossteffan, E., Gueux, A., Guillaudeau, J., Guillou, G., Jolly, O., Lachaussée, N., Lafont, M., Lagadec, V., Lamoureux, J., Lauga, B., Lebreton, B., Lecuyer, E., Lehodey, J.-P., Leroux, C., L'Helguen, S., Macé, E., Maria, E., Mousseau, L., Nowaczyk, A., Pineau, P., Petit, F., Pujo-Pay, M., Raimbault, P., Rimmelin-Maury, P., Rouaud, V., Sauriau, P.-G., Sultan, E., Susperregui, N., 2018. Dynamics of particulate organic matter composition in coastal systems: Forcing of spatio-temporal variability at multi-systems scale. Progress in Oceanography 162, 271–289. https://doi.org/10.1016/j.pocean.2018.02.026

Ljungström, G., Claireaux, M., Fiksen, Ø., Jørgensen, C., 2020. Body size adaptions under climate change: zooplankton community more important than temperature or food abundance in model of a zooplanktivorous fish. Marine Ecology Progress Series 636, 1–18. https://doi.org/10.3354/meps13241

Lowry, O.H., Rosebrough, N.J., Farr, A.L., Randall, R.J., 1951. Protein measurement with the Folin phenol reagent. Journal of Biological Chemistry 193, 265–275.

Maguer, J.-F., L'helguen, S., Le Corre, P., 2000. Nitrogen Uptake by Phytoplankton in a Shallow Water Tidal Front. Estuarine, Coastal and Shelf Science 51, 349–357. https://doi.org/10.1006/ecss.2000.0678

Major, Y., Kifle, D., Niedrist, G.H., Sommaruga, R., 2017. An isotopic analysis of the phytoplankton–zooplankton link in a highly eutrophic tropical reservoir dominated by cyanobacteria. Journal of Plankton Research 39, 220–231. https://doi.org/10.1093/plankt/fbx007

Mason, R.P., Reinfelder, J.R., Morel, F.M.M., 1995. Bioaccumulation of mercury and methylmercury. Water Air Soil Pollut 80, 915–921. https://doi.org/10.1007/BF01189744

Mauchline, J., 1998. The biology of Calanoid copepods. In: Blaxter, J.H.S., Southward, A.J., Tyler, P.A.(Eds.), Advances in Marine Biology, 245–292. Academic Press, San Diego, USA.

Mayot, N., D'Ortenzio, F., Uitz, J., Gentili, B., Ras, J., Vellucci, V., Golbol, M., Antoine, D., Claustre, H., 2017. Influence of the Phytoplankton Community Structure on the Spring and Annual Primary Production in the Northwestern Mediterranean Sea. Journal of Geophysical Research: Oceans 122, 9918–9936. https://doi.org/10.1002/2016JC012668

Mayzaud, P., Chanut, J., Ackman, R., 1989. Seasonal changes of the biochemical composition of marine particulate matter with special reference to fatty acids and sterols. Marine Ecology Progress Series 56, 189–204. https://doi.org/10.3354/meps056189

Montoya, J.P., Carpenter, E.J., Capone, D.G., 2002. Nitrogen fixation and nitrogen isotope abundances in zooplankton of the oligotrophic North Atlantic. Limnology and Oceanography 47, 1617–1628. https://doi.org/10.4319/lo.2002.47.6.1617

Morris, M.J., Hopkins, T.L., 1983. Biochemical composition of crustacean zooplankton from the eastern Gulf of Mexico. Journal of Experimental Marine Biology and Ecology 69, 1–19.

Motwani, N.H., Gorokhova, E., 2013. Mesozooplankton Grazing on Picocyanobacteria in the Baltic Sea as Inferred from Molecular Diet Analysis. PLOS ONE 8, e79230. https://doi.org/10.1371/journal.pone.0079230

Onodera, T., Kanaya, G., Hatamoto, M., Kohzu, A., Iguchi, A., Takimoto, Y., Yamaguchi, T., Mizuochi, M., Syutsubo, K., 2018. Evaluation of trophic transfer in the microbial food web during sludge degradation based on 13C and 15N natural abundance. Water Research 146, 30–36. https://doi.org/10.1016/j.watres.2018.09.016

Ostrom, P. H., Fry, B., 1993. Sources and cycling of organic matter within modern and prehistoric food webs. Organic geochemistry, 785-798. Springer, Boston, MA.

Pantoja, S., Repeta, D.J., Sachs, J.P., Sigman, D.M., 2002. Stable isotope constraints on the nitrogen cycle of the Mediterranean Sea water column. Deep Sea Research Part I: Oceanographic Research Papers 49, 1609–1621. https://doi.org/10.1016/S0967-0637(02)00066-3

Parnell, A.C., Phillips, D.L., Bearhop, S., Semmens, B.X., Ward, E.J., Moore, J.W., Jackson, A.L., Grey, J., Kelly, D.J., Inger, R., 2013. Bayesian stable isotope mixing models. Environmetrics 24, 387–399. https://doi.org/10.1002/env.2221

Peterson, B.J., Howarth, R.W., Garritt, R.H., 1985. Multiple stable isotopes used to trace the flow of organic matter in estuarine food webs. Science 227, 1361–1363. https://doi.org/10.1126/science.227.4692.1361

Phillips, D.L., Inger, R., Bearhop, S., Jackson, A.L., Moore, J.W., Parnell, A.C., Semmens, B.X., Ward, E.J., 2014. Best practices for use of stable isotope mixing models in food-web studies. Canadian Journal of Zoology 92, 823–835. https://doi.org/10.1139/cjz-2014-0127

Pinnegar, J.K., Polunin, N.V.C., 1999. Differential fractionation of δ13C and δ15N among fish tissues: implications for the study of trophic interactions. Functional Ecology 13, 225–231. https://doi.org/10.1046/j.1365-2435.1999.00301.x

Post, D.M., 2002. Using Stable Isotopes to Estimate Trophic Position: Models, Methods, and Assumptions. Ecology 83, 703–718. https://doi.org/10.1890/0012-9658(2002)083[0703:USITET]2.0.CO;2

Postel, L., Fock, H., Hagen, W., 2000. 4 - Biomass and abundance, In: Harris, R., Wiebe, P., Lenz, J., Skjoldal, H.R., Huntley, M. (Eds.), ICES Zooplankton Methodology Manual. Academic Press, London, pp. 83–192. https://doi.org/10.1016/B978-012327645-2/50005-0

Raimbault, P., Diaz, F., Pouvesle, W., Boudjellal, B., 1999. Simultaneous determination of particulate organic carbon, nitrogen and phosphorus collected on filters, using a semi-automatic wet-oxidation method. Marine Ecology Progress Series 180, 289.

Raimbault, P., Garcia, N., Cerutti, F., 2008. Distribution of inorganic and organic nutrients in the South Pacific Ocean; evidence for long-term accumulation of organic matter in nitrogen-depleted waters. Biogeosciences 5, 281–298. https://doi.org/10.5194/bg-5-281-2008

Rau, G., Teyssie, J., Rassoulzadegan, F., Fowler, S., 1990. C-13/C-12 and N-15/N-14 variations among size-fractionated marine particles - implications for their origin and trophic relationships. Marine Ecology Progress Series 59(1/2), 33–38.

Ríos, A.F., Fraga, F., Pérez, F.F., Figueiras, F.G., 1998. Chemical composition of phytoplankton and Particulate Organic Matter in the Ría de Vigo (NW Spain). Scientia Marina 62 (3), 257–271 https://doi.org/10.3989/scimar.1998.62n3257

Rolff, C., 2000. Seasonal variation in δ13C and δ15N of size-fractionated plankton at a coastal station in the northern Baltic proper. Marine Ecology Progress Series 203, 47–65. https://doi.org/10.3354/meps203047

Ryther, J.H., 1969. Photosynthesis and Fish Production in the Sea. Science 166, 72–76. https://doi.org/10.1126/science.166.3901.72

Schartup, A.T., Qureshi, A., Dassuncao, C., Thackray, C.P., Harding, G., Sunderland, E.M., 2018. A Model for Methylmercury Uptake and Trophic Transfer by Marine Plankton. Environmental Science & Technology 52, 654–662. https://doi.org/10.1021/acs.est.7b03821

Sommer, F., Stibor, H., Sommer, U., Velimirov, B., 2000. Grazing by mesozooplankton from Kiel Bight, Baltic Sea, on different sized algae and natural seston size fractions. Marine Ecology Progress Series 199, 43–53. https://doi.org/10.3354/meps199043

Sommer, U., Stibor, H., Katechakis, A., Sommer, F., Hansen, T., 2002. Pelagic food web configurations at different levels of nutrient richness and their implications for the ratio fish production:primary production, in: Vadstein, O., Olsen, Y. (Eds.), Sustainable Increase of Marine Harvesting: Fundamental Mechanisms and New Concepts. Springer Netherlands, Dordrecht, pp. 11–20. https://doi.org/10.1007/978-94-017-3190-4_2

Søreide, J.E., Hop, H., Carroll, M.L., Falk-Petersen, S., Hegseth, E.N., 2006. Seasonal food web structures and sympagic–pelagic coupling in the European Arctic revealed by stable isotopes and a two-source food web model. Progress in Oceanography 71, 59–87. https://doi.org/10.1016/j.pocean.2006.06.001

Tamelander, T., Kivimäe, C., Bellerby, R.G.J., Renaud, P.E., Kristiansen, S., 2009. Base-line variations in stable isotope values in an Arctic marine ecosystem: effects of carbon and nitrogen uptake by phytoplankton. Hydrobiologia 630, 63–73. https://doi.org/10.1007/s10750-009-9780-2

Tao, Y., Yu, J., Liu, X., Xue, B., Wang, S., 2018. Factors affecting annual occurrence, bioaccumulation, and biomagnification of polycyclic aromatic hydrocarbons in plankton food webs of subtropical eutrophic lakes. Water Research 132, 1–11. https://doi.org/10.1016/j.watres.2017.12.053

Tedetti, M., Tronczynski, J., 2019. HIPPOCAMPE cruise, RV Antea. https://doi.org/10.17600/18000900

Tedetti, M., Tronczynski, J., Carlotti, J.F., Pagano, M., Ben Ismail, S., Sammari, C., Bel Hassen, M., Desboeufs, K., Poindron, C., Chifflet, S., Bellaaj Zouari, A., Abdennadher, M., Amri, S., Bănaru, D., Ben Abdallah, L., Bhairy, N., Boudriga, I., Bourin, A., Brach-Papa, C., Briant, N., Cabrol, L., Chevalier, C., Chouba, L., Coudray, S., Daly Yahia, M. N., de Garidel Thoron, T., Dufour, A., Dutay, J-C., Espinasse, B., Fierro-González, P., Fornier, M., Garcia, N., Giner, F., Guigue, C., Guilloux, L., Hamza, A., Heimbürger-Boavida, L-E., Jacquet, S., Knoery, J., Lajnef, R., Makhlouf Belkahia, N., Malengros, D., Martinot, P.L., Bosse, A., Mazur, J-C., Meddeb, M., Misson, B., Pringault, O., Quéméneur, M., Radakovitch, O., Raimbault, P., Ravel, R., Rossi, R., Rwawi, C., Sakka Hlaili, A., Tesán-Onrubia, J.A., Thomas, B., Thyssen, M., Zaaboub, N., Garnier, C., 2023. Contamination of planktonic food webs in the Mediterranean Sea: Setting the

frame for the MERITE-HIPPOCAMPE oceanographic cruise (spring 2019). Marine Pollution Bulletin. In press in this special issue.

Tiano, M., Tronczyński, J., Harmelin-Vivien, M., Tixier, C., Carlotti, F., 2014. PCB concentrations in plankton size classes, a temporal study in Marseille Bay, Western Mediterranean Sea. Marine Pollution Bulletin 89, 331–339. https://doi.org/10.1016/j.marpolbul.2014.09.040

Tiselius, P., Fransson, K., 2016. Daily changes in δ15N and δ13C stable isotopes in copepods: equilibrium dynamics and variations of trophic level in the field. Journal of Plankton Research 38, 751–761. https://doi.org/10.1093/plankt/fbv048

Trimble, S.M., Baskaran, M., 2005. The role of suspended particulate matter in 234Th scavenging and 234Th-derived export fluxes of POC in the Canada Basin of the Arctic Ocean. Marine Chemistry 96, 1–19. https://doi.org/10.1016/j.marchem.2004.10.003

Vander Zanden, M.J.V., Rasmussen, J.B., 2001. Variation in δ15N and δ13C trophic fractionation: Implications for aquatic food web studies. Limnology and Oceanography 46, 2061–2066. https://doi.org/10.4319/lo.2001.46.8.2061

Wainright, S.C., Fry, B., 1994. Seasonal variation of the stable isotopic compositions of coastal marine plankton from Woods Hole, Massachusetts and Georges Bank. Estuaries 17, 552–560. https://doi.org/10.2307/1352403

Wu, Y., Wang, W.-X., 2011. Accumulation, subcellular distribution and toxicity of inorganic mercury and methylmercury in marine phytoplankton. Environmental Pollution, Nitrogen Deposition, Critical Loads and Biodiversity 159, 3097–3105. https://doi.org/10.1016/j.envpol.2011.04.012

Yang, G., Li, C., Guilini, K., Wang, X., Wang, Y., 2017. Regional patterns of δ13C and δ15N stable isotopes of size-fractionated zooplankton in the western tropical North Pacific Ocean. Deep Sea Research Part I: Oceanographic Research Papers 120, 39–47. https://doi.org/10.1016/j.dsr.2016.12.007

Yılmaz, A.Z., Besiktepe, S., 2010. Annual variations in biochemical composition of size fractionated particulate matter and zooplankton abundance and biomass in Mersin Bay, NE Mediterranean Sea. Journal of Marine Systems 81, 260–271. https://doi.org/10.1016/j.jmarsys.2010.01.002

Figure captions

Figure 1. Location of the ten sampling stations of the MERITE-HIPPOCAMPE campaign in the Mediterranean Sea (April-Mai 2019).

Figure 2. Boxplot of the concentrations of A) proteins, B) carbohydrates, C) lipids (µg mg^{-1} DW) and D) energy content (E_i) (kJ g^{-1} DW) in the different plankton size-fractions (fractions between 0.7 and 60 µm in green and > 60 µm in orange) for all stations combined. H = Kruskal–Wallis non-parametric test and the associated p-value for the respective biochemical compounds: H = 43.5, $p < 0.0001$; H = 110.6, $p < 0.001$; H = 41.8, $p < 0.0001$ and H = 51.7, $p < 0.0001$. Mean values with different letters are significantly different ($p < 0.05$). The mean and median values are represented by a cross and a horizontal line, respectively, and the box length is defined as the interquartile range. The minimum and maximum values are represented by whiskers. Mean values with different post-hoc letters are significantly different ($p < 0.05$).

Figure 3. Boxplot of the concentrations of A, B) proteins, C, D) carbohydrates, E, F) lipids (µg mg^{-1} DW) and G, H) energy content (E_i) (kJ g^{-1} DW) in the phyto- (fractions between 0.7 and 60 µm – in green) and zooplankton (fractions between 60 and 500 µm – in orange) fractions for each station. H = Kruskal–Wallis non-parametric test and the associated p-value for the respective biochemical compounds for phytoplankton (H = 43.4, $p < 0.0001$; H = 30.6, $p < 0.0001$; H = 34.9, $p < 0.0001$ and H = 42.9, $p < 0.0001$) and for zooplankton (H = 43.8, $p < 0.0001$; H = 22.9, $p < 0.006$; H = 38.8, $p < 0.0001$ and H = 38.8, $p < 0.0001$). Stations are grouped by geographical area: St1, St2, St3 and St4 for the Northern coast, St9, St10 and St11 for the offshore area, and St15, St17 and St19 for the Southern coast. The mean and median values were represented by a cross and a horizontal line, respectively, and the box length is defined as the interquartile range. The minimum and maximum values are represented by whiskers. Mean values with different post-hoc letters are significantly different ($p < 0.05$).

Figure 4. Total amount of energy provided by plankton (E_T in kJ m^{-3}) for each of the size-fractions by station. Stations are grouped by geographical area: St1, St2, St3 and St4 for the Northern coast, St9, St10 and St11 for the offshore area, and St15, St17 and St19 for the Southern coast.

Figure 5. Mean (± standard error, SE) stable isotope compositions ($\delta^{13}C$ and $\delta^{15}N$ values, ‰) in the different plankton size-fractions for all stations combined. Green dots correspond to the phytoplankton size-fractions (from 0.7 to 60 µm), while the orange dots correspond to zooplankton size-fractions (> 60 µm).

Figures 6. Boxplot of the A, B) $\delta^{13}C$ and C, D) $\delta^{15}N$ values (‰) in the phyto- (fractions between 0.7 and 60 µm – in green) and zooplankton (fractions between 60 and 500 µm – in orange) fractions for each station. Stations are grouped by geographical area: St1, St2, St3 and St4 for the Northern coast, St9, St10 and St11 for the offshore area, and St15, St17 and St19 for the Southern coast. Kruskall-Wallis non-parametric test were performed for A) (H = 25.5, $p < 0.05$), C) (H = 24.1, $p < 0.05$) and D) (H = 33.5, $p < 0.0001$), and one-way

ANOVA test was performed for B) ($F = 4.4$, $p < 0.0001$). The mean and median values are represented by a cross and a horizontal line, respectively, and the box length is defined as the interquartile range. The minimum and maximum values are represented by whiskers. Mean values with different post-hoc letters are significantly different ($p < 0.05$).

Figure 7. Boxplot of the trophic levels (TL) of the zooplankton size-fractions (60 to > 2000 µm). The median value is represented by a horizontal line and the box length is defined as the interquartile range. The minimum and maximum values are represented by whiskers. One-way ANOVA test ($F = 5.17$, $p = 0.001$). Superscript letters represent Newman-Keuls post-hoc groups and values with the different letters are significantly different ($p < 0.05$).

Figure 8. Trophic levels (TL) of the zooplankton size-fractions (60 to > 2000 µm) and mean TL weighted by their biomass (TL_B) for each station. Stations are gathered by geographical area: St1, St2, St3 and St4 for the Northern coast, St9, St10 and St11 for the offshore area, and St15, St17 and St19 for the Southern coast.

Figure 9. Relative contributions of 0.7–2.7 µm (pico-), 2.7–20 µm (nano-), and 20–60 µm (microplankton) as food resources for three zooplankton size-fractions. Arrows indicate the trophic transfer between pico-POM nano-POM, and micro-POM fractions and zooplankton size fractions: 60–500 µm (in green), 500–2000 µm (in blue) and > 2000 µm (in orange). Their thickness is proportional to relative contribution in percentage, indicated close to the corresponding arrow.

Table 1. Suspended particulate matter and plankton dry weight (SPM_{DW} and $Plankton_{DW}$, in mg DW L^{-1}) for the different plankton size-fractions and stations, as well as total chlorophyll *a* concentration (TChl*a*, µg L^{-1}) for the > 0.7-µm fraction. Kruskal-Wallis test and the associated p-value for SPM_{DW} ($H = 23.15$, $p < 0.0001$) and $Plankton_{DW}$ ($H = 28.51$, $p < 0.0001$). Superscript letters represent rank comparison groups and values with different letters are significantly different ($p < 0.05$). St = station, SE = standard-error, n = number of samples.

Figures

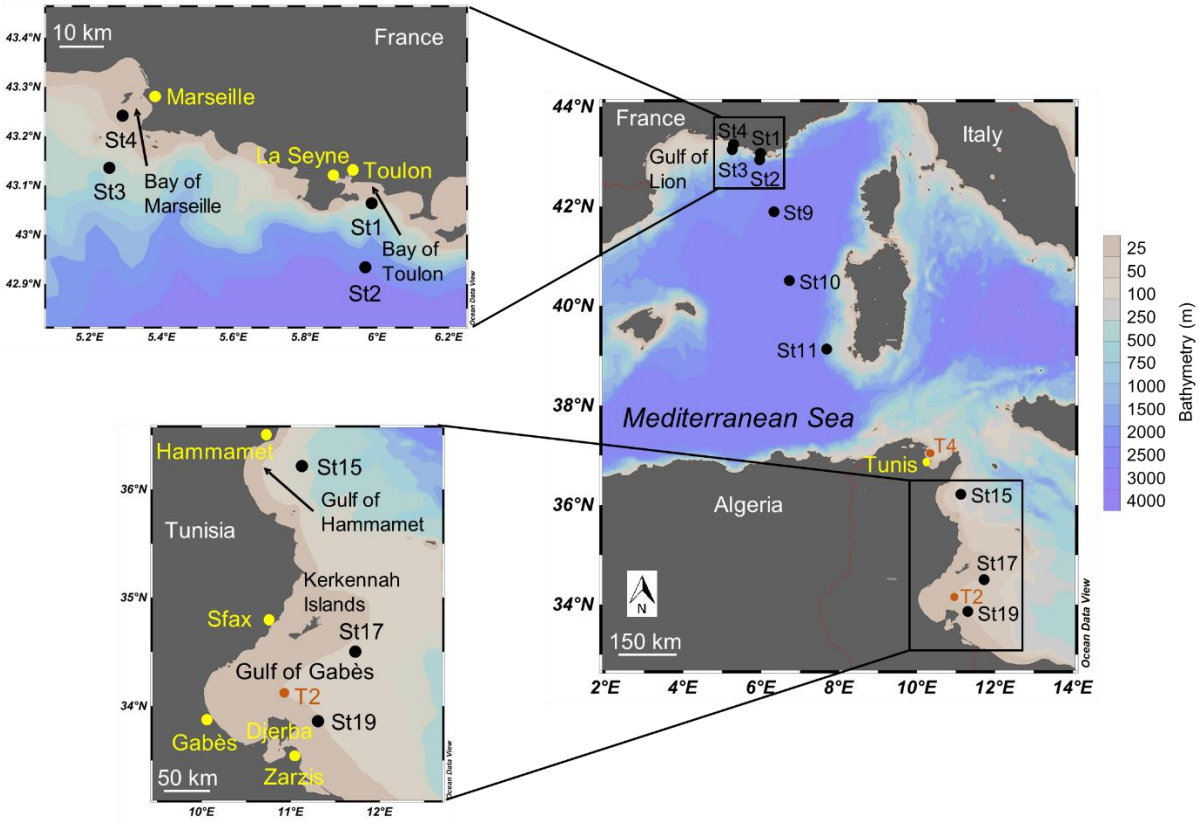

Figure 1

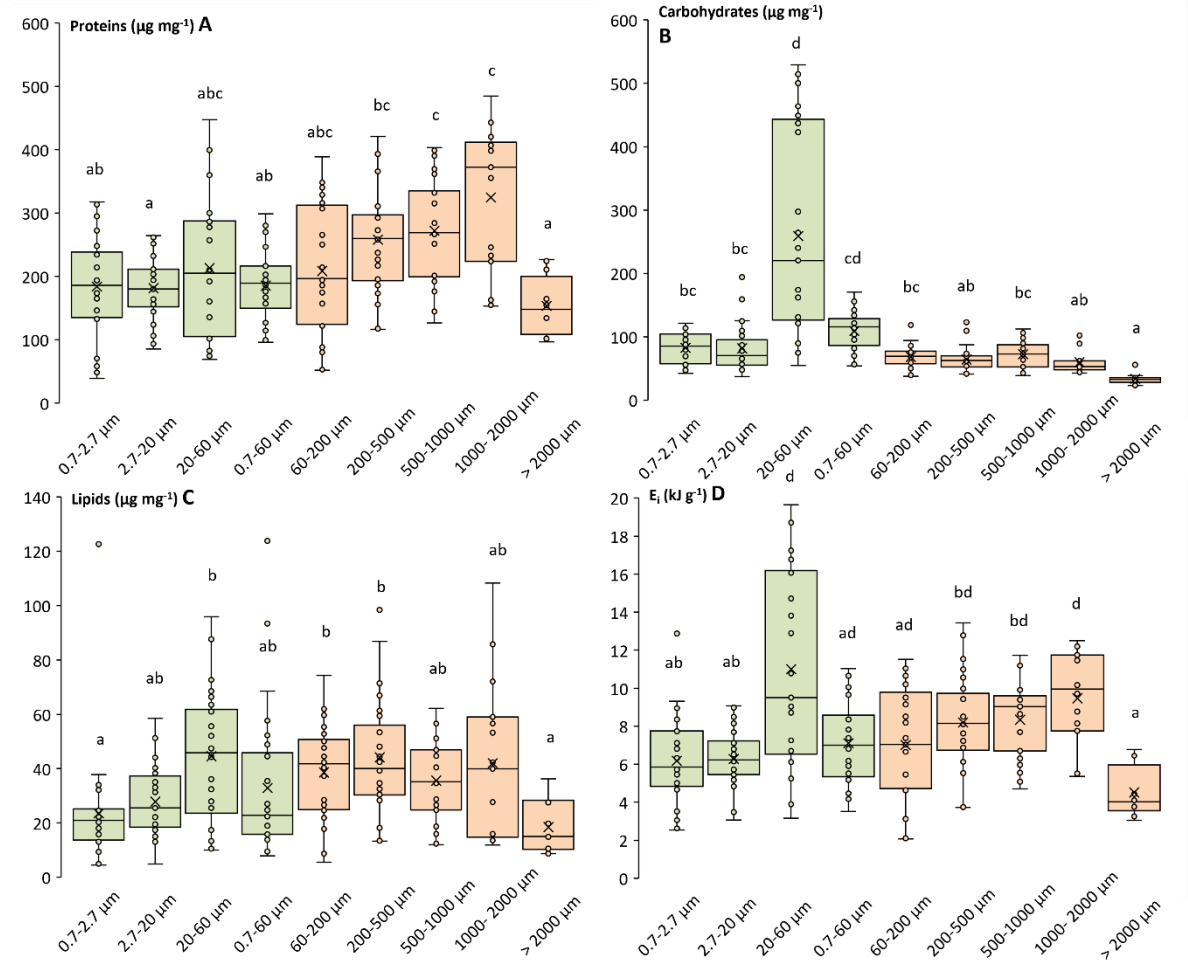
Proteins (µg mg-1) A
Carbohydrates (µg mg-1) B
Lipids (µg mg-1) C
Ei (kJ g-1) D
0.7-2.7 µm
2.7-20 µm
20-60 µm
0.7-60 µm
60-200 µm
200-500 µm
500-1000 µm
1000- 2000 µm
> 2000 µm

Figure 2

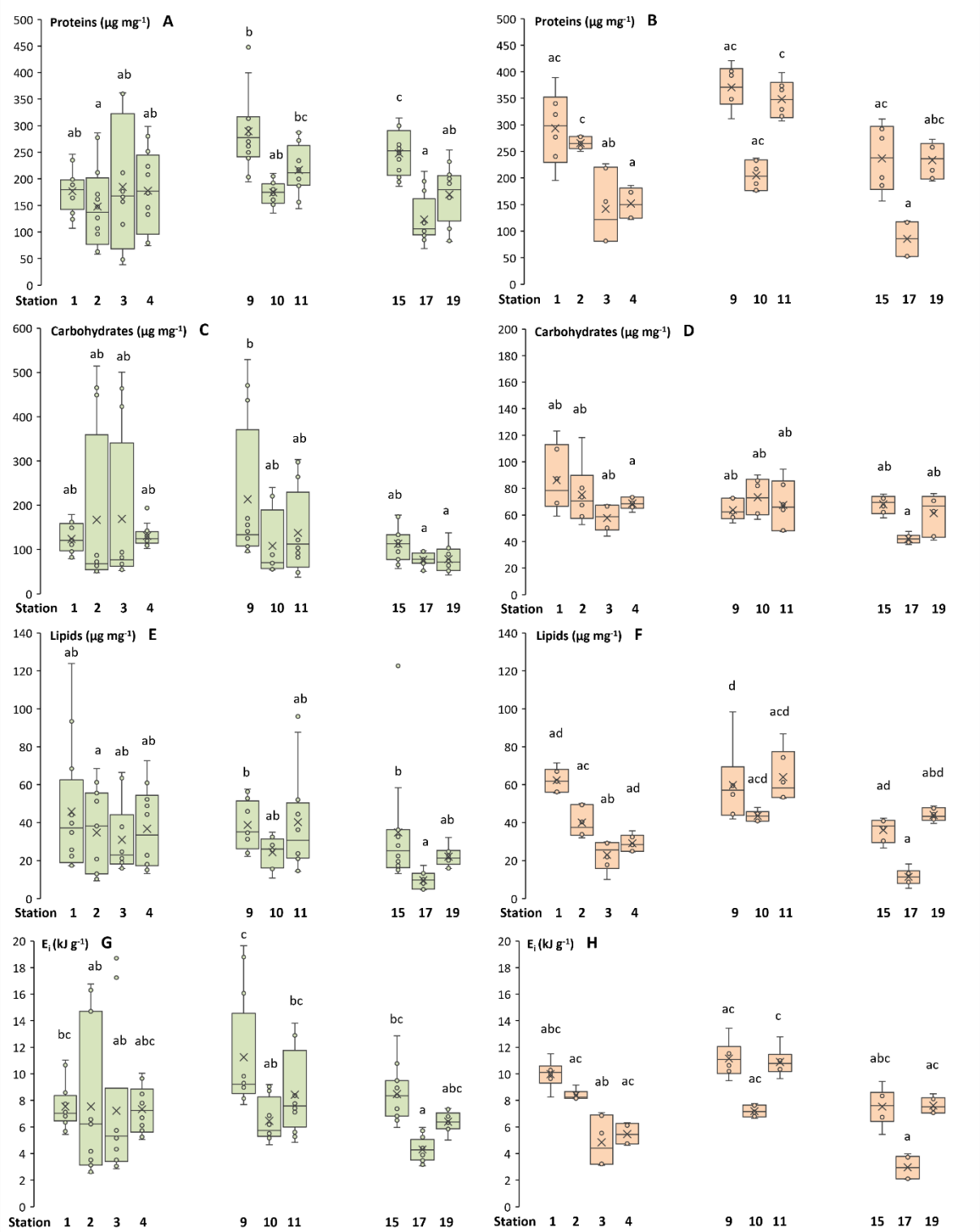
Proteins (µg mg-1) A
Proteins (µg mg-1) B
Carbohydrates (µg mg-1) C
Carbohydrates (µg mg-1) D
Lipids (µg mg-1) E
Lipids (µg mg-1) F
Ei (kJ g-1) G
Ei (kJ g-1) H
Station 1 2 3 4 9 10 11 15 17 19

Figure 3

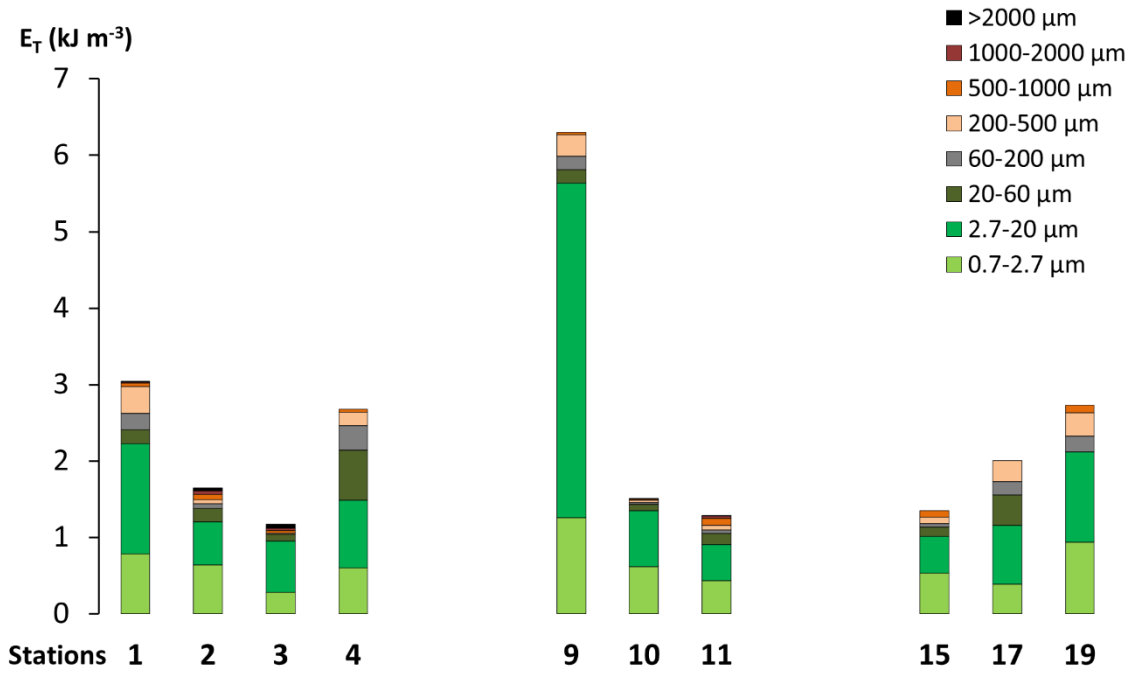

1258

1259 **Figure 4**

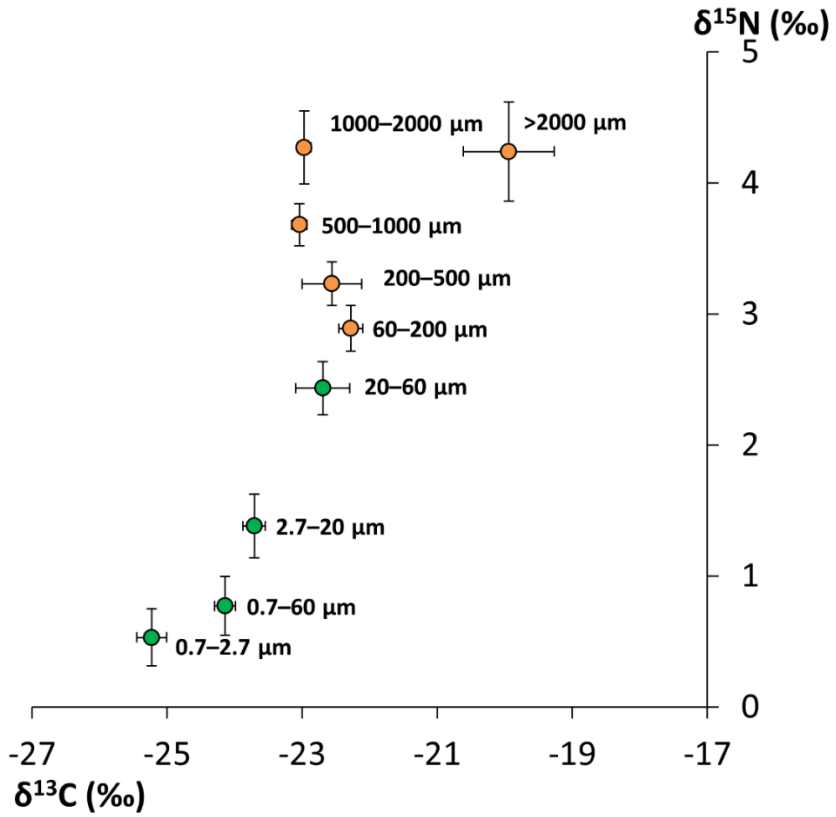
δ15N (‰)
5
4
3
2
1
0
1000–2000 µm
>2000 µm
500–1000 µm
200–500 µm
60–200 µm
20–60 µm
2.7–20 µm
0.7–60 µm
0.7–2.7 µm
-27
-25
-23
-21
-19
-17
δ13C (‰)

Figure 5

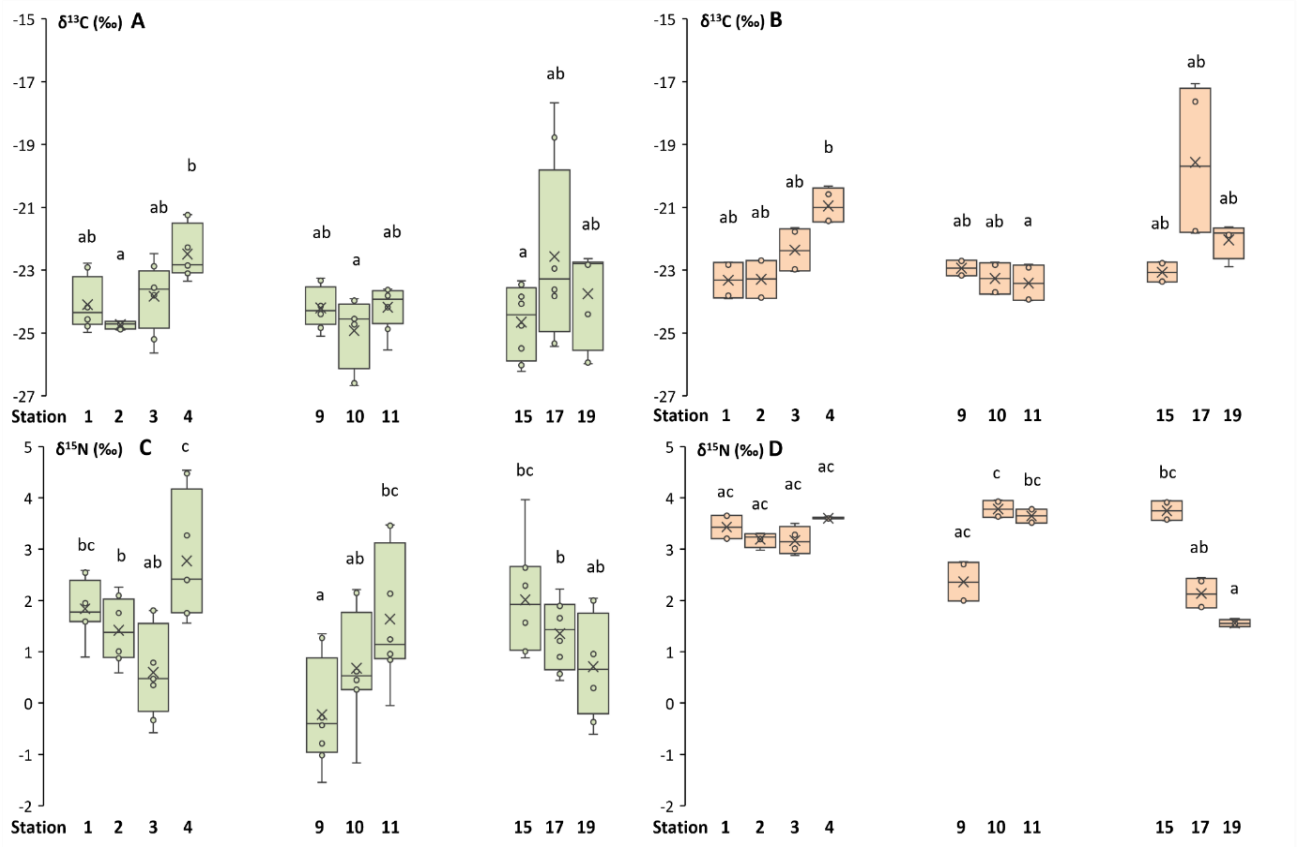

Figure 6

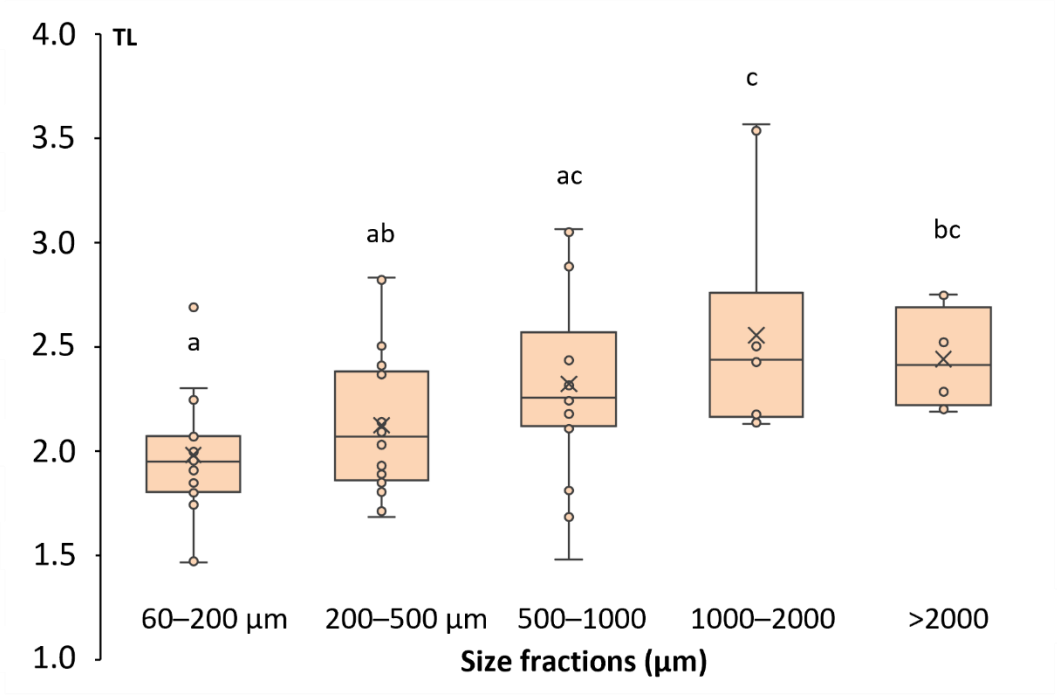
TL
4.0
3.5
3.0
2.5
2.0
1.5
1.0
a
ab
ac
c
bc
60–200 µm
200–500 µm
500–1000
1000–2000
>2000
Size fractions (µm)

Figure 7

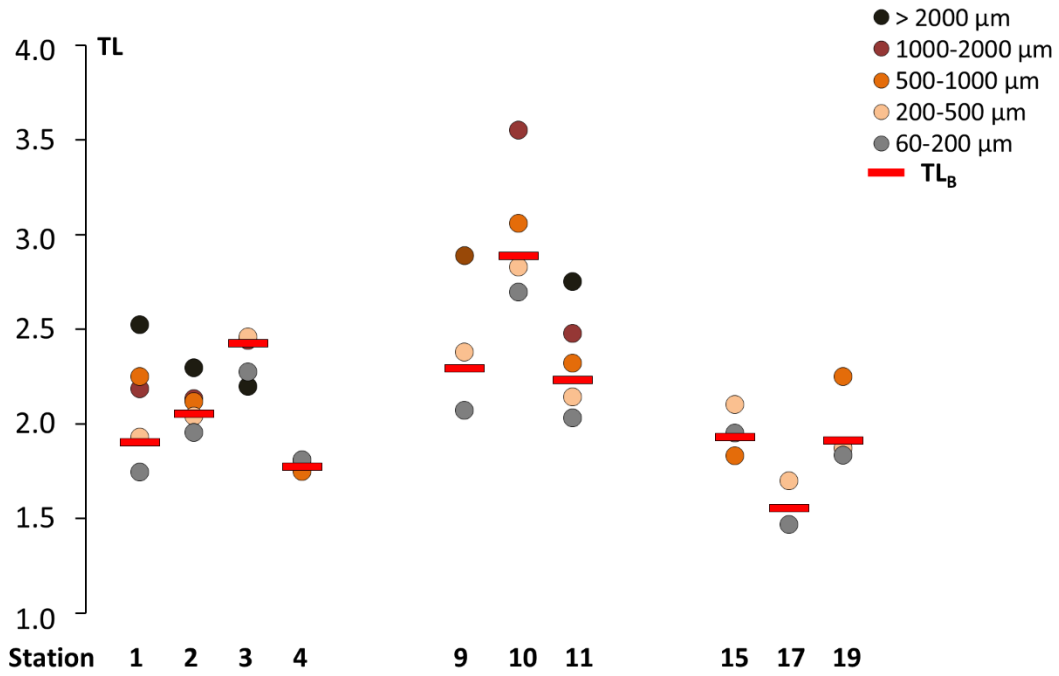
TL
4.0
3.5
3.0
2.5
2.0
1.5
1.0
Station
1
2
3
4
9
10
11
15
17
19
> 2000 µm
1000-2000 µm
500-1000 µm
200-500 µm
60-200 µm
TL_B

Figure 8

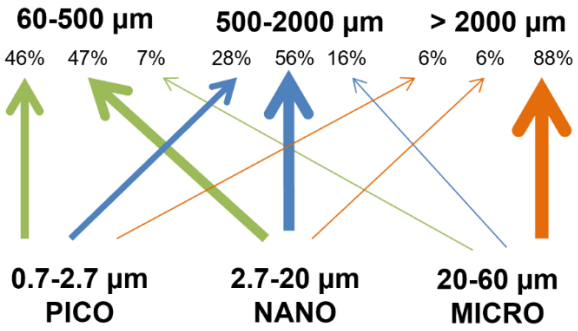

1274

1275 **Figure 9**

1276

1277 **Tables**

1278 **Table 1.**

Stations	St1	St2	St3	St4	St9	St10	St11	St15	St17	St19	n	Mean ± SE	
Size-fractions							SPM_{DW} (mg DW L^{-1})						
0.7–2.7 µm	0.11	0.23	0.09	0.11	0.14	0.12	0.06	0.05	0.07	0.16	10	0.11 ± 0.02	ab
2.7–20 µm	0.24	0.09	0.12	0.11	0.53	0.13	0.09	0.07	0.23	0.17	10	0.18 ± 0.04	bc
20–60 µm	0.03	0.01	0.00	0.11	0.01	0.01	0.01	0.01	0.11	0.11	10	0.04 ± 0.02	a
0.7–60 µm	0.35	0.32	0.21	0.22	0.67	0.25	0.15	0.12	0.29	0.34	10	0.29 ± 0.05	c
TChl*a* (> 0.7 µm) (µg L^{-1})	0.77	0.38	0.68	0.98	1.54	0.55	0.38	0.67	0.21	1.45	10	0.76 ± 0.14	
							$Plankton_{DW}$ (mg DW L^{-1})						
60–200 µm	0.020	0.007	0.002	0.068	0.017	0.003	0.004	0.006	0.083	0.029	10	0.024 ± 0.027	ab
200–500 µm	0.037	0.007	0.002	0.028	0.023	0.004	0.005	0.010	0.072	0.038	10	0.023 ± 0.021	ab
500–1000 µm	0.005	0.007	0.004	0.007	0.004	0.002	0.009	0.009	0.002	0.011	10	0.006 ± 0.003	b
1000–2000 µm	0.002	0.005	0.007	0.002	0.0002	0.001	0.002	0.001		0.0000	10	0.002 ± 0.002	a
> 2000 µm	0.0004	0.005	0.013			0.0001	0.0004	0.001		0.0002	10	0.003 ± 0.005	a
Sum													
60–>2000 µm	0.064	0.031	0.028	0.105	0.044	0.011	0.020	0.026	0.157	0.078	50	0.057 ± 0.019	

1279